bcl-2 (16). Moreover, the interaction between PKCη and cyclin E is carefully regulated, and it correlates with the inactive form of the cyclin E/Cdk2 complex (17). An atypical PKCζ blocks the phosphorylation of Akt in breast cancer cells (18). These data strongly suggest that PKC is involved in the proliferation, differentiation and death of breast cancer cells.

The mitogen-activated protein kinase (MAPK) family consists of extracellular signal-regulated kinase (ERK) MAPK, c-jun NH_2-terminal kinase (JNK) and p38. The protein kinase cascade is activated in response to various external stimuli and transfers extracellular signals to the nuclei. Various cellular responses, such as proliferation, differentiation and cell death, are controlled by the regulation of gene expression by MAPK. ERK MAPK is considered to function in cell proliferation and differentiation. It is a focus of research relating to carcinogenesis, particularly because of activation by downstream signaling cascades of growth factors (19,20). It has also been shown in breast cancer cells, that HER2 and PKCδ are involved in the activation of ERK MAPK induced by estrogen (21). Furthermore, angiotensin II induced, in a dosage-dependent manner, proliferation of breast cancer cells and acceleration of phosphorylation of ERK MAPK, secondary to translocation of PKCα, ß and δ. Therefore, it is assumed that there is a close relationship between PKC and MAPK. However, the potential role of PKC or MAPK as mediators of the antineoplaston effects in breast cancer cells have not yet been investigated in detail. If this relationship could be clarified in breast cancer cells, antineoplaston treatment could be an effective therapy for breast cancer patients.

The present study examined the effects of antineoplaston A10 on PKC and ERK MAPK signaling, as well as in the regulation of the cell cycle in the SKBR-3 human breast cancer cell line. Interestingly, we found that A10 caused G_1 arrest in SKBR-3 cells, and that PKCα and ERK MAPK were closely involved in the inhibition of cell proliferation.

Materials and methods

Materials. Antineoplaston A10 was provided by Dr S.R. Burzynski (Burzynski Research Institute, Inc.). PD98059 and Gö6976 were obtained from Alexis Corporation (San Diego, CA).

Cell culture and cell proliferation studies. The SKBR-3 breast cancer cell line, was obtained from the American Type Culture Collection (ATCC) (Manassas, VA), and was cultured in Dulbecco's modified Eagle's medium (DMEM) supplemented with 10% fetal bovine serum (FBS) at 37˚C in an atmosphere of 5% CO_2.

Treatment of antineoplaston A10. To assess the effect of A10 on cell proliferation, concentrations of 1, 3 or 10 mg/ml were added to SKBR-3 cells in 6-well plates and incubated for 24-72 h. Cells were then suspended by treatment with 0.05% trypsin and counted using a hemocytometer.

Flow cytometry. Cells were fixed with 70% ethanol, stained with propidium iodide (1 mg/ml), and examined for changes in the cell cycle distribution using flow cytometry (FACScan, Becton-Dickinson, CA).

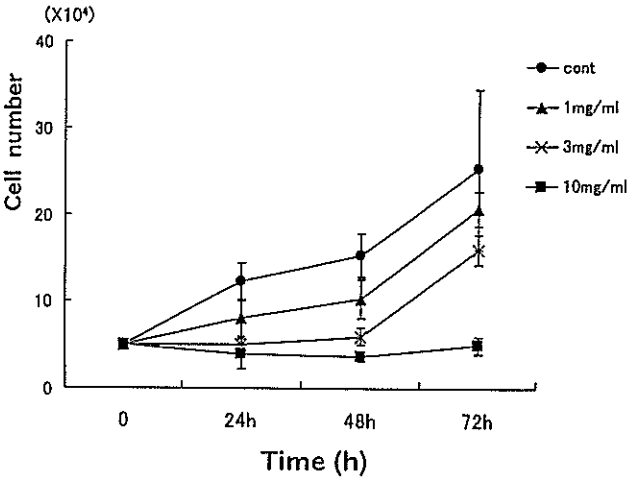

Figure 1. Effect of A10 on SKBR-3 cell growth. Different concentrations of A10 (1, 3 or 10 mg/ml) were added to SKBR-3 cells in 6-well plates for different incubation periods. The cell number was determined by hemocytometer counting. Data are expressed as the mean ± SE of three independent experiments.

Western blot analysis. Lysis buffer (50 mM Tris-HCl, pH 7.4, 1% NP-40, 0.25% Na-deoxycholate, 150 mM NaCl, 1 mM Na_3VO_4, 1 mM PMSF, 1 mM NaF, 1 µg/ml pepstatin) was added to SKBR-3 cells, and SDS-polyacrylamide gel slab electrophoresis was performed, followed by blotting onto a nitrocellulose membrane. Membranes were blocked for 1 h using tris-buffered saline (TBS) containing 5% milk and 0.1% Tween-20 and then incubated for 24 h with one of the following primary antibodies; anti-PKCα, δ, ε, ι, θ and ζ (1:1,000, Transduction Laboratories, Lexington, KY), anti-ERK MAPK (1:1,000, phosphospecific antibody and total antibody, New England Biolabs, Beverly, MA), anti-p16 (1:1,000, Santa Cruz Biotechnology, Santa Cruz, CA), anti-p21 (1:1,000, Santa Cruz Biotechnology), anti-p27 (1:1,000, Santa Cruz Biotechnology), anti-cyclin D1 (1:1,000, PharMingen, San Diego, CA), anti-cyclin E (1:1,000, PharMingen), anti-phosphospecific-retinoblastoma (Rb) (Ser807/811) (1:1,000, Cell Signaling Technology, Beverly, MA) and anti-ß-actin (1:1,000, Sigma, Saint Louis, MO). After washing three times with TBS containing 0.1% Tween-20, the membrane was incubated for 60 min with the secondary antibody (1:2,000, anti-mouse or anti-rabbit horseradish peroxidase, Bio-Rad, CA). Bands were detected using the enhanced chemiluminescence (ECL) Western blot detection system (Amersham Biosciences, Buckinghamshire, UK).

Statistical analysis. Statistical analysis was performed using the Student's t-test. A level of $p<0.05$ was considered statistically significant.

Results

A10 inhibits proliferation of SKBR-3 breast cancer cells. A10 caused the dose-dependent inhibition of SKBR-3 cells (Fig. 1). When compared to the control, cells incubated for 72 h with 1, 3 or 10 mg/ml A10 underwent 36 and 80% cell growth inhibition, respectively.

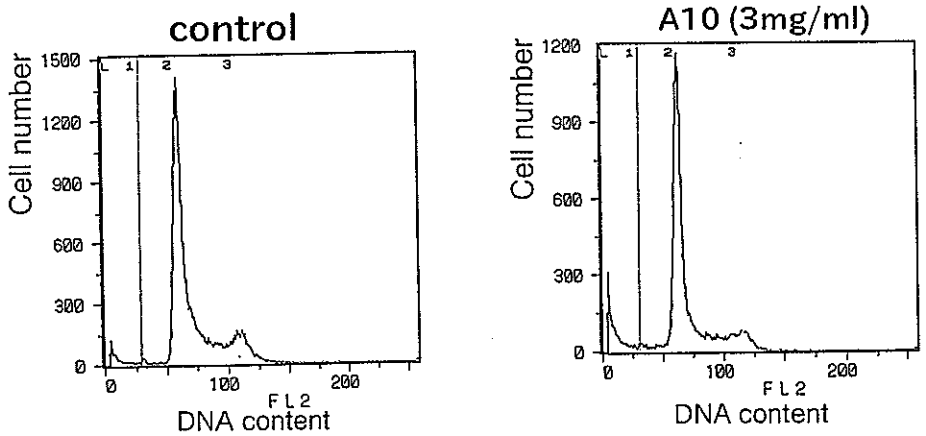

Phase	Control	A10 (3mg/ml)
G_0/G_1	44%	59%
S	48%	37%
G_2/M	8%	5%

Figure 2. A10-induced changes in the cell cycle. SKBR-3 cells were treated with 3 mg/ml A10 for 24 h, and then fixed with 70% ethanol, stained with propidium iodide (1 mg/ml), and examined for changes in the cell cycle distribution using flow cytometry. A representative experiment is shown. Similar results were obtained in two additional experiments.

Effects of A10 on cell cycle distribution. The cell growth curves and the flow cytometry results suggested that A10 inhibited the growth of SKBR-3 cells, and increased the proportion of cells in the G_0/G_1 phase, that is, they caused G_1 arrest. Analysis of the cell cycle showed that in the group without A10, 44% of the cells were in the G_0/G_1 phase, and 8% at the G_2/M phase. However, in the 3 mg/ml A10 group after 24 h, 59% of the cells were in the G_0/G_1 phase and 5% at the G_2/M phase, indicating that the percentage of G_0/G_1-phase cells had increased markedly (Fig. 2).

Effect of A10 on p16, p21, p27, cyclins and Rb. It has been suggested that SKBR-3 cells undergo G_1 arrest after A10 treatment, therefore we examined the expression of cell cycle regulators that are essential for G_0/G_1 progression. We focused on changes in p16, p21, p27, cyclin D1, cyclin E protein expression and phosphorylation of Rb protein. As a result, expression of p16 and p21 protein was increased at 12 h after the administration of A10 (Fig. 3), while there was no change in the expression of cyclin D1, cyclin E and p27 protein (data not shown). Furthermore, the phosphorylation of Rb at Ser807/811 was inhibited 24 h after A10 was administered (Fig. 3).

A10-induced changes in PKC expression and effect of the classical PKC inhibitor Gö6976. Since PKC is strongly related to cell growth we next investigated how A10 affects this enzyme. The expression of PKCα decreased at 30 min after 3 mg/ml A10 was added, but expression of other PKC proteins was unchanged (Fig. 4A). These results suggest that PKCα is

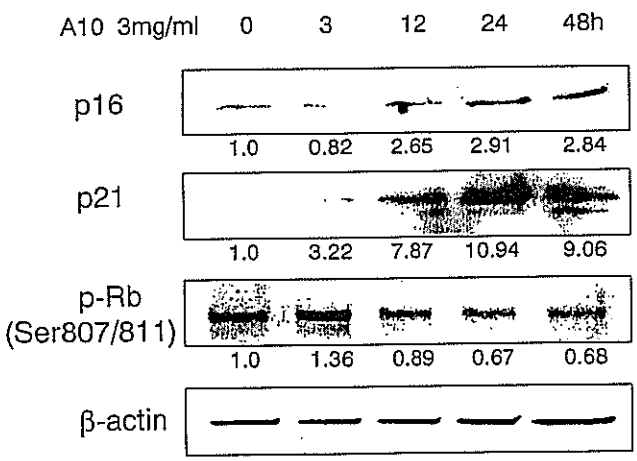

Figure 3. Effect of A10 on p16, p21 protein expression and Rb phosphorylation. SKBR-3 cells were treated with 3 mg/ml A10. Between 0 and 48 h, the expression of p16, p21 protein and Rb phosphorylation was examined by Western blotting. Similar results were observed in two additional experiments. Values indicate the density of the band.

involved in the control of SKBR-3 cell proliferation by A10. The potential role of PKCα isozymes in the A10-mediated control of SKBR-3 cell proliferation was evaluated using a classical PKC inhibitor, Gö6976. As SKBR-3 cells do not express PKCß or PKCγ (23), Gö6976 acted on them as a specific PKCα inhibitor. SKBR-3 cells were treated with vehicle (control), Gö6976 (3 μM) alone, or with a combination of A10 (3 mg/ml) and Gö6976 (3 μM). After 24 h, the cells

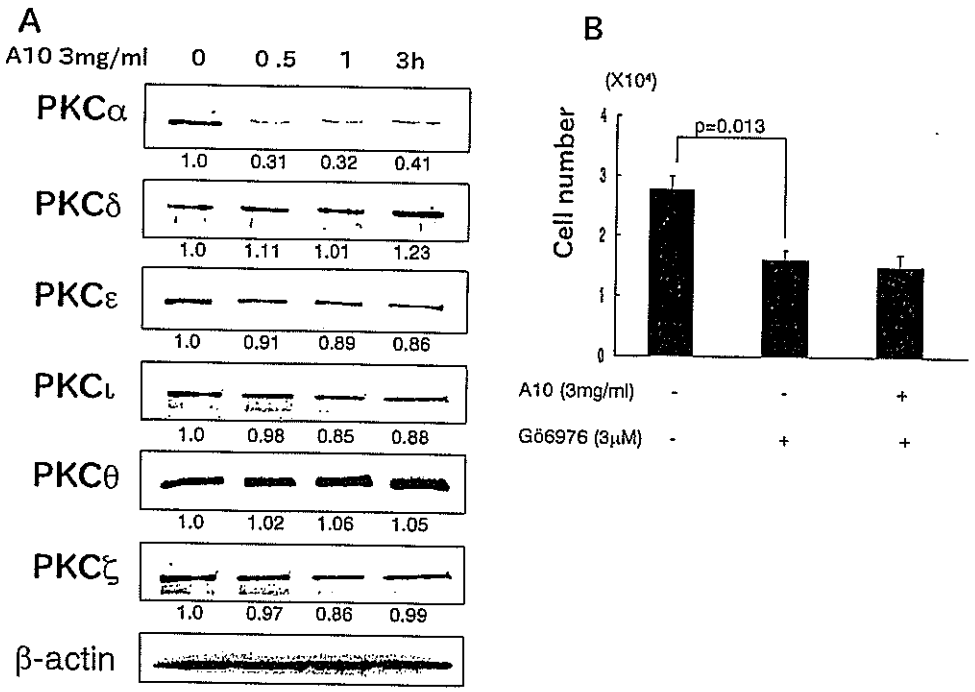

Figure 4. A10-induced changes in PKC isozymes and effect of Gö6976. (A) SKBR-3 cells were treated with A10 (3 mg/ml) for different periods, as detailed in the figure. Expression of PKC isozymes was determined by Western blotting using specific anti-PKC antibodies. Similar results were observed in two additional experiments. Values indicate the density of the band. (B) SKBR-3 cells were treated with vehicle (control), Gö6976 (3 μM) alone or with a combination of A10 (3 mg/ml) and Gö6976 (3 μM). After 24 h, the cells were suspended by treatment with 0.05 % trypsin and counted. Data are expressed as the mean ± SE of three independent experiments.

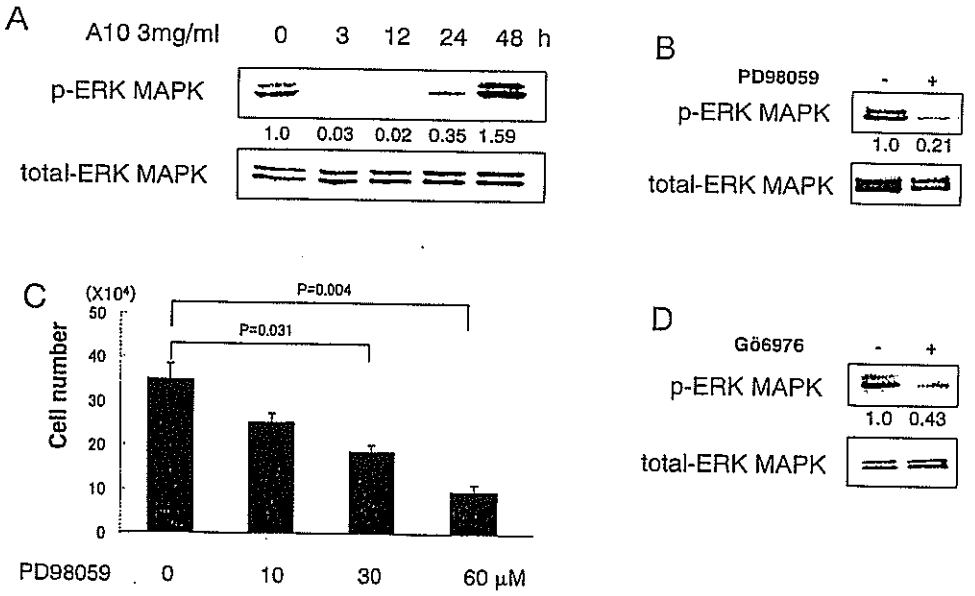

Figure 5. Effect of A10 on ERK MAPK phosphorylation. (A) SKBR-3 cells were treated with 3 mg/ml A10 for different times, as indicated in the figure. Phospho- and total ERK MAPK was assessed by Western blotting. Similar results were observed in two additional experiments. Values indicate the density of the band. (B) Effect of PD98059 on ERK MAPK phosphorylation. Cells were treated with PD98059 (30 μM), and ERK MAPK phosphorylation was assessed 12 h later by Western blotting. Similar results were observed in two additional experiments. Values indicate the density of the band. (C) SKBR-3 cells were treated with different concentrations of PD98059 for 24 h, and the cell number was determined by hemocytometer counting. Data are expressed as the mean ± SE of three independent experiments. (D) Effect of Gö6976 on ERK MAPK phosphorylation. Cells were treated with Gö6976 (3 μM), and ERK MAPK phosphorylation was assessed 12 h later by Western blotting. Similar results were observed in two additional experiments. Values indicate the density of the band.

were suspended by treatment with 0.05% trypsin and counted. Interestingly, Gö6976 produced a significant reduction in the cell number compared to the control (p=0.013). This effect was similar in the presence of A10 (Fig. 4B). Therefore, these results strongly suggest that PKCα is closely involved in the A10-induced inhibition of SKBR-3 cell growth.

Effect of A10 on MAPK. The changes induced by A10 in ERK MAPK were assessed to investigate the pathway downstream from PKC. The addition of A10 produced no change in the total ERK MAPK protein in SKBR-3 cells, but the expression of phosphospecific ERK MAPK decreased markedly 3 h after the 3 mg/ml concentration was added (Fig. 5A). These data suggest that ERK MAPK was closely involved in the A10-induced inhibition of SKBR-3 cell growth. Confirmation of whether ERK MAPK was involved in SKBR-3 cell growth was obtained by adding PD98059, (an inhibitor of mitogen-activated protein kinase kinase [MEK] 1 which is responsible for ERK MAPK activation), to cell cultures and analyzing any changes in cell growth. The expression of phosphorylated ERK MAPK decreased markedly at 12 h after the administration of PD98059, confirming ERK MAPK phosphorylation inhibition by PD98059 (Fig. 5B). The groups receiving 30 or 60 μM PD98059, showed 46.6 and 72.3% growth inhibition, respectively (compared with the control), indicating significant dose-dependent cell growth inhibition ($p<0.05$) (Fig. 5C). To establish a potential role for PKCα in this process, we assessed the effect of Gö6976 on ERK MAPK phosphorylation. Treatment with Gö6976 inhibited ERK MAPK phosphorylation fully after 12 h (Fig. 5D). These results strongly suggested a role for PKCα in the activation of ERK MAPK by A10.

Discussion

The antineoplaston A10 markedly inhibited the proliferation of the breast cancer cell line, SKBR-3, by causing cell-cycle arrest in the G_1 phase. Our findings are consistent with a previous report that demonstrated that antineoplaston induced G_1 arrest and differentiation of human hepatocellular carcinoma cells (24). The mechanism of G_1 arrest by A10 has been suggested to occur at the level of PKC expression and ERK MAPK phosphorylation, since both are important regulators of G_1/S transition. In fact, the expression of PKCα protein decreased markedly on treatment with A10, while other PKC isozymes remained unchanged. On the basis of these results, it is tempting to speculate that PKC, especially PKCα, is involved in the control of G_1/S transition in SKBR-3 cells, probably through controlling essential regulators of G_1/S progression. We used the classical PKC inhibitor, Gö6976, to further investigate how PKCα is involved in the A10-induced inhibition of SKBR-3 cell growth. Interestingly, Gö6976 impaired cell growth significantly. Inhibition of PKCα function, either by pharmacological inhibition with Gö6976 or by reduced protein expression on treatment with A10, impaired the growth of SKBR-3 cells markedly. The lack of an inhibitory effect caused by Gö6976 in A10-treated cells could be related to the low levels of PKCα present after A10 treatment. This would strongly reinforce the concept that PKC plays a major role in the control of cell proliferation in this cell model.

Next, to demonstrate the presence of a signal downstream from PKC, we analyzed MAPK expression. A10 produced little or no change in the expression of the ERK MAPK protein, but its phosphorylation was inhibited 3 h post exposure. This result suggests that ERK MAPK is closely involved in the A10-induced inhibition of SKBR-3 cell growth. This was also supported by the finding that the ERK MAPK-specific inhibitor, PD98059, inhibited cell growth significantly. Moreover, a PKCα blockade with Gö6976 inhibited ERK MAPK phosphorylation, a clear indication that PKCα is an upstream regulator of ERK MAPK in this cell model. Similar findings have been reported in other cell types (25-27).

Among signals downstream of ERK MAPK, control of the cell cycle is considered most important as it is directly related to the control of cell growth. The G_1 phase of the cell cycle is controlled by the cyclin/cyclin dependent kinase (cdk) complex, or inhibitor of cyclin/cdk complex such as p16 or p21 through phosphorylation of Rb (28,29). We therefore assessed the effect of A10 on the expression of cyclins, p16, p21 proteins, and the phosphorylation of Rb. A10 increased the expression of p16 and p21, and inhibited the phosphorylation of Rb at Ser807/811. We speculate that the precise cause of the A10-induced G_1 arrest of SKBR-3 cells was the inhibition of Rb protein phosphorylation associated with the up-regulation of p16 and p21 protein expression. However, in the present study, A10 did not induce changes in cyclin expression, suggesting that G_1 arrest in these cells might be caused by a reduction of cdk kinase activity or some other unidentified factor.

These data lead us to conclude that the exposure of SKBR-3 breast cancer cells to A10 caused the down-regulation of PKCα protein expression, resulting in inhibition of ERK MAPK phosphorylation, increasing p16 and p21 protein expression, with the resultant inhibition of Rb phosphorylation leading to G_1 arrest. Our data indicate the existence of a pathway in which A10 arrests SKBR-3 cells in the G_1 phase via PKC and MAPK. This is the first report, to our knowledge, describing the relationship between antineoplaston and PKC or MAPK. In conclusion, this study suggests that once the mechanism underlying the antineoplaston antitumor effect is fully elucidated, it may provide an effective therapy for breast cancer patients.

References

1. Burzynski SR: Antineoplastons: biochemical defence against cancer. Physiol Chem Phys 8: 275-279, 1976.
2. Burzynski SR: The present state of antineoplaston research (1). Integr Cancer Ther 3: 47-58, 2004.
3. Tsuda H, Sata M, Kumabe T, Uchida M and Hara H: The preventive effect of antineoplaston AS2-1 on HCC recurrence. Oncol Rep 10: 391-397, 2003.
4. Tsuda H, Sata M, Ijuuin H, Kumabe T, Uchida M, Ogou Y, Akagi Y, Shirouzu K, Hara H and Nakashima Y: A novel strategy for remission induction and maintenance in cancer therapy. Oncol Rep 9: 65-68, 2002.
5. Tsuda H, Sata M, Kumabe T, Hara H, Eriguchi N, Sugita Y and Nagamatsu H: Quick response of advanced cancer to chemo-radiation therapy with antineoplastons. Oncol Rep 5: 597-600, 1998.
6. Kumabe T, Tsuda H, Uchida M, Ogoh Y, Hayabuchi N, Sata M, Nakashima O and Hara H: Antineoplaston treatment for advanced hepatocellular carcinoma. Oncol Rep 5: 1363-1367, 1998.
7. Badria F, Mabed M, El-Awadi M, Abou-Zeid L, Al-Nashar E and Hawas S: Immune modulatory potentials of antineoplaston A-10 in breast cancer patients. Cancer Lett 157: 57-63, 2000.
8. Takai Y, Kishimoto A, Inoue M and Nishizuka Y: Studies on acyclic nucleotide-independent protein kinase and its proenzyme in mammalian tissues. I. Purification and characterization of an active enzyme from bovine cerebellum. J Biol Chem 252: 7603-7609, 1977.
9. Nishizuka Y: The molecular heterogeneity of protein kinase C and its implications for cellular regulation. Nature 334: 661-665, 1984.

10. Nishizuka Y: Intracellular signaling hydrolysis of phospholipids and activation of protein kinase C. Science 258: 607-614, 1992.
11. Nishizuka Y: Protein kinase C and lipid signaling for sustained cellular responses. FASEB J 9: 484-496, 1995.
12. Musashi M: The roll of protein kinase C isoform in cell proliferation and apoptosis. Int J Hematol 72: 12-19, 2000.
13. Akkaraju GR and Basu A: Overexpression of protein kinase C-η attenuates caspase activation and tumor necrosis factor-α-induced cell death. Biochem Biophys Res Commun 279: 103-107, 2000.
14. Basu A: Differential sensitivity of breast cancer cells to tumor necrosis factor-α: involvement of protein kinase C. Biochem Biophys Res Commun 280: 883-891, 2001.
15. Gauthier ML, Torretto C, Ly J, Francescutti V and O'Day DH: Protein kinase Cα negatively regulates cell spreading and motility in MDA-MB-231 human breast cancer cells downstream of epidermal growth factor receptor. Biochem Biophys Res Commun 307: 839-846, 2003.
16. Soh JW, Lee YS and Weinstein IB: Effects of regulatory domains of specific isoforms of protein kinase C on growth control and apoptosis in MCF-7 breast cancer cells. J Exp Ther Oncol 3: 115-126, 2003.
17. Shtutman M, Hershko T, Maissel A, Fima E and Livneh E: PKCη associates with cyclin E/Cdk2 complex in serum-starved MCF-7 and NIH-3T3 cells. Exp Cell Res 286: 22-29, 2003.
18. Mao M, Fang X, Lu Y, Lapushin R, Bast RC Jr and Mills GB: Inhibition of growth-factor-induced phosphorylation and activation of protein kinase B/Akt by atypical protein kinase C in breast cancer cells. Biochem J 2: 475-482, 2000.
19. Cowley S, Paterson H, Kemp P and Marshall CJ: Activation of MAP kinase kinase is necessary and sufficient for PC12 differentiation and for transformation of NIH 3T3 cells. Cell 77: 841-852, 1994.
20. Mansour SJ, Matten WT, Hermann AS, Candia JM, Rong S, Fukasawa K, Vande Woude GF and Ahn NG: Transformation of mammalian cells by constitutively active MAP kinase kinase. Science 265: 966-970, 1994.
21. Keshamouni VG, Mattingly RR and Reddy KB: Mechanism of 17-ß-estradiol-induced Erk1/2 activation in breast cancer cells. A role for HER2 AND PKC-δ. J Biol Chem 277: 22558-22565, 2002.
22. Greco S, Muscella A, Elia MG, Salvatore P, Storelli C, Mazzotta A, Manca C and Marsigliante S: Angiotensin II activates extracellular signal regulated kinases via protein kinase C and epidermal growth factor receptor in breast cancer cells. J Cell Physiol 196: 370-377, 2003.
23. Le XF, Marcelli M, McWatters A, Nan B, Mills GB, O'Brian CA and Bast RC Jr: Heregulin-induced apoptosis is mediated by down-regulation of Bcl-2 and activation of caspase-7 and is potentiated by impairment of protein kinase C α activity. Oncogene 20: 8258-8269, 2001.
24. Tsuda H, Iemura A, Sata M, Uchida M, Yamana K and Hara H: Inhibitory effect of antineoplaston A10 and AS2-1 on human hepatocellular carcinoma. Kurume Med J 43: 137-147, 1996.
25. Schonwasser DC, Marais RM, Marshall CJ and Parker PJ: Activation of the mitogen-activated protein kinase/extracellular signal-regulated kinase pathway by conventional, novel and atypical protein kinase C isotypes. Mol Cell Biol 18: 790-798, 1998.
26. Yoon YM, Oh CD, Kim DY, Lee YS, Park JW, Huh TL, Kang SS and Chun JS: Epidermal growth factor negatively regulates chondrogenesis of mesenchymal cells by modulating the protein kinase C-α, Erk-1 and p38 MAPK signaling pathways. J Biol Chem 275: 12353-12359, 2000.
27. Lo LW, Cheng JJ, Chiu JJ, Wung BS, Liu YC and Wang DL: Endothelial exposure to hypoxia induces Egr-1 expression involving PKC α-mediated Ras/Raf-1/ERK1/2 pathway. J Cell Physiol 188: 304-312, 2001.
28. Meyerson M and Harlow E: Identification of G1 kinase activity for cdk6, a novel cyclin D partner. Mol Cell Biol 14: 2077-2086, 1994.
29. Draetta G: Cell cycle control in eukaryotes: molecular mechanisms of cdc2 activation. Trends Biochem Sci 15: 378-383, 1990.

0022-3565/05/3152-888–895$20.00
THE JOURNAL OF PHARMACOLOGY AND EXPERIMENTAL THERAPEUTICS

JPET 315:888–895, 2005

Vol. 315, No. 2
86827/3057515
Printed in U.S.A.

Functional Analysis of Organic Cation Transporter 3 Expressed in Human Placenta

Ryoko Sata, Hisakazu Ohtani, Masayuki Tsujimoto, Hideyasu Murakami, Noriko Koyabu, Takanori Nakamura, Takeshi Uchiumi, Michihiko Kuwano, Hideaki Nagata, Kiyomi Tsukimori, Hitoo Nakano, and Yasufumi Sawada

Department of Medico-Pharmaceutical Sciences (R.S., H.O., M.T., H.M., N.K., Y.S.), Graduate School of Pharmaceutical Sciences, Kyushu University, Fukuoka, Japan; and Departments of Biochemistry (T.N., T.U., M.K.) and Reproduction and Gynecology (H.Nag., K.T., H.Nak.), Graduate School of Medical Sciences, Kyushu University, Fukuoka, Japan

Received March 23, 2005; accepted August 2, 2005

ABSTRACT

The aim of this study is to investigate the placental transport mechanism of cationic compounds by comparison of the uptake of an organic cation into human placental basal membrane vesicles (BLMVs) with that into organic cation transporter 3 (OCT3)-expressing cells. Reverse transcription-polymerase chain reaction analysis demonstrated that OCT3 is the only OCT isoform expressed in the human placenta. The function of OCT3 was investigated by measuring the uptake of 1-methyl-4-phenylpyridinium (MPP^+) into human embryonic kidney (HEK)293 cells stably expressing OCT3 (HEK/OCT3 cells). The OCT3-mediated uptake of MPP^+ was sodium- and chloride-independent and saturable, with a Michaelis constant (K_m) of 82.5 μM. The OCT3-mediated uptake was inhibited by various cationic drugs in a concentration-dependent manner but not by anionic compounds, such as *p*-aminohippuric acid and captopril, or a zwitterion, carnitine. Western blotting analysis of membrane vesicles prepared from human term placenta revealed that OCT3 is expressed only in BLMVs but not in microvillous membrane vesicles. The uptake of MPP^+ into BLMVs was membrane potential-dependent and saturable, with a K_m value of 51.8 μM, which is similar to that in HEK293/OCT3 cells. The inhibitory spectrum of various compounds on MPP^+ uptake by BLMVs was also similar to that in HEK293/OCT3 cells. These results suggest that OCT3 is expressed on the basal membrane of human trophoblast cells and plays an important role in the placental transport of cationic compounds.

Throughout gestation, the placenta plays an important role in regulating the supply of nutrients to the fetus, excretion of metabolic waste products from the fetus, and so on. In the placenta, trophoblast cells, which face the maternal blood, are considered to be the functional entity of the blood-placental barrier. Various transporters have been identified on both microvillous membrane and basal membrane, which face the maternal and fetal side, respectively, of trophoblast cells and are considered to regulate the exchange of various materials between mother and fetus.

Monoamines, including serotonin and norepinephrine, and cationic drugs, such as cimetidine and procainamide, are transported by organic cation transport systems in the kidney and liver (Koepsell, 1998; Kamisako et al., 1999; Dresser et al., 2000; Hohage and Gerhardt, 2000; Suzuki and Sugiyama, 2000). Rat organic cation transporter 1 (rOCT1) was first cloned from rat kidney as a component of the organic cation transport system (Gründemann et al., 1994). Whereas mouse and rat OCT1 are expressed in both liver and kidney (Gründemann et al., 1994; Schweifer and Barlow, 1996), hOCT1 is mainly expressed in the liver (Gorboulev et al., 1997; Zhang et al., 1999). It has also been shown by immunohistochemical study that rOCT1 is expressed on the sinusoidal membrane of hepatocytes (Meyer-Wentrup et al., 1998) and the basolateral membrane of renal tubular epithelium (Karbach et al., 2000; Sugawara-Yokoo et al., 2000).

rOCT2 was cloned as a homolog of rOCT1 from rat kidney (Okuda et al., 1996). Unlike hOCT1, OCT2 is expressed predominantly in the kidney (Okuda et al., 1996; Gorboulev et al., 1997) and is localized on the basolateral membrane of

This study was supported in part by a Grant-in-aid for Young Scientists (A) from the Ministry of Education, Culture, Sports, Science and Technology of Japan.
Article, publication date, and citation information can be found at http://jpet.aspetjournals.org.
doi:10.1124/jpet.105.086827.

ABBREVIATIONS: rOCT, rat organic cation transporter; OCT, organic cation transporter; hOCT, human organic cation transporter; BLMV, human placental basolateral membrane vesicle; MPP^+, 1-methyl-4-phenylpyridinium; RT-PCR, reverse transcription-polymerase chain reaction; HEK, human embryonic kidney; BBMV, human placental microvillous membrane vesicle; PBS, phosphate-buffered saline; ALP, alkaline phosphatase; ANOVA, analysis of variance; PAH, *p*-aminohippuric acid.

renal proximal tubules (Karbach et al., 2000; Sugawara-Yokoo et al., 2000).

Organic cation transporter 3 (OCT3) was first cloned from rat placenta (Kekuda et al., 1998), and its orthologues were also cloned from humans and mice (Gründemann et al., 1998; Verhaagh et al., 1999). Because hOCT3 has high affinity for monoamines, such as histamine, it is also designated as extraneuronal monoamine transporter (Gründemann et al., 1998). In contrast to OCT1 and 2, OCT3 is widely expressed (Kekuda et al., 1998; Verhaagh et al., 1999), although its expression is particularly high in the placenta (Verhaagh et al., 1999). Recently, it has been reported that pregnant OCT3-knockout mice exhibit reduced accumulation of MPP^+ in the embryo compared with pregnant control mice, although the MPP^+ concentration in placenta and amniotic fluid was not affected, suggesting that OCT3 mediates the transport of MPP^+ from the placenta to the fetus but not from the maternal circulation (Zwart et al., 2001). These findings emphasize the importance of OCT3 in the placental transfer of cationic compounds, although its subcellular localization in the placenta and other tissues still remains unknown.

Besides OCTs, various transporters of organic cations have been identified in the human placenta. The expression of OCTN1, a member of a new subfamily of OCTs, has been reported in the human placenta, but its subcellular localization remains to be identified (Tamai et al., 1997). Another OCTN, OCTN2, has been demonstrated to be expressed on the maternal side (microvillous membrane) of trophoblast cells by Western blotting (Lahjouji et al., 2004). An organic cation/proton antiporter, norepinephrine transporter, serotonin transporter, and P-glycoprotein have been found on the microvillous membrane of trophoblast cells (Ganapathy et al., 2000; Ushigome et al., 2003), but the identity of the transporter of organic cations on the basolateral membrane remains unknown. The aim of this study is to investigate the placental transport mechanism of cationic compounds by comparison of the uptake of a model organic cation into human placental basal membrane vesicles (BLMVs) with that into OCT3-expressing cells.

Materials and Methods

Materials and Reagents. [^{3}H]MPP^+ (85.0 Ci/mmol), [^{3}H]quinine (14.5 Ci/mmol), and [^{3}H]dihydroalprenolol (60 Ci/mmol) were purchased from American Radiolabeled Chemicals (St. Louis, MO). [^{14}C]Tetraethylammonium (2.4 Ci/mmol) was purchased from PerkinElmer Life and Analytical Sciences (Boston, MA). [^{3}H]Theophylline (18.5 Ci/mmol) was purchased from Moravek Biochemicals (Brea, CA). Anti-OCT3 goat polyclonal antibody OCT3 (C-14) was purchased from Santa Cruz Biotechnology, Inc. (Santa Cruz, CA). Horseradish peroxidase-labeled anti-goat IgG antibody was purchased from Valeant Pharmaceuticals (Costa Mesa, CA). All other chemicals used in this study were commercial products of reagent grade.

Functional Expression of OCT3 in Mammalian Cells. Human OCT3 cDNA was obtained from human kidney total RNA by RT-PCR using KOD-plus-polymerase (Toyobo Engineering, Osaka, Japan). Sequence analysis revealed that the obtained OCT3 cDNA was 300 base pairs shorter than the OCT3 cloned previously (GenBank accession no. AJ001417; Gründemann et al., 1998). The missing part of the OCT3 cDNA was obtained by PCR using an Advantage-GC Genomic PCR kit (BD Biosciences Clontech, Palo Alto, CA) and human liver cDNA (BD Biosciences Clontech) under the following conditions: 1) 94°C × 3 min; 2) 94°C × 30 s, 68°C × 3 min (35 cycles); and 3) 68°C × 3 min. The full-length OCT3 cDNA was generated using the restriction enzyme BglII and subcloned into pIRESneo vector.

Sequencing of the cDNA was carried out with an ABI Prism BigDye Terminator Cycle Sequencing kit and 373 DNA sequencer (Applied Biosystems, Foster City, CA), and the sequence was analyzed by Sequencing Analysis 3.0 (Applied Biosystems). Sequence analysis showed that there was a G1260A mutation compared with the sequence already published by Gründemann et al. (1998), but it was a silent mutation.

An aliquot of 1 μg of OCT3/pIRESneo vector was transfected into HEK293 cells with LipofectAMINE 2000 Reagent (Invitrogen, Tokyo, Japan). After incubation for 24 h, cells were released by trypsin treatment and cultured in minimal essential medium containing 500 μg/ml geneticin. The cells were grown for 3 to 4 weeks and then used as HEK293 cells stably expressing OCT3 (HEK/OCT3 cells).

Preparation of Human Placental BLMVs and Microvillous Membrane Vesicles (BBMVs). Human placental BLMVs were prepared by the method of Inuyama et al. (2002) with minor modifications. Human term placentas from uncomplicated pregnancies were obtained within 15 min after vaginal or cesarean delivery and placed in 0.9% NaCl. After removal of the cord, amniochorion, and decidua, placental tissue was cut from the maternal side and washed in phosphate-buffered saline (PBS) (−). Tissue was stirred in PBS (−) for 30 min and collected on a nylon mesh. The filtrate was washed three times with ice-cold 50 mM Tris-HCl, pH 7.4, collected on a 250-μm pore size nylon mesh, and divided into several equal portions. Each portion was sonicated in 100 ml of the same Tris buffer using a 3/4-inch-high gain probe for 10 s at 240 W (Vibra-cell; Sonics and Materials, Newtown, CT). The suspensions were kept on ice. The sonication procedure selectively removes any remaining microvillous membrane. Sonicated tissue was collected on the mesh, washed three times with 5 mM Tris-HCl, pH 7.4, and then stirred gently for 60 min in the same buffer. Tissue was then collected on the nylon mesh and washed again in the same buffer. This procedure disrupts and removes the intracellular components, thus exposing the basolateral membranes. Tissue portions of 25 to 30 g were resuspended in approximately 100 ml of 50 mM Tris-HCl, pH 7.4, containing 10 mM EDTA and 250 mM sucrose and incubated for 30 min with occasional stirring. The portions were then sonicated twice for 20 s at 250 W to release the basolateral membranes. The suspensions were strained through nylon mesh, and the supernatant was centrifuged at 3430*g* for 10 min to remove debris. The supernatant from this spin was recentrifuged at 80,000*g* for 40 min to yield the basolateral membrane pellet, which was resuspended, using a Dounce homogenizer in 25 mM HEPES-Tris, pH 7.4, containing 1 mM EDTA and 275 mM sucrose. This fraction was further purified by centrifugation on a discontinuous gradient of 10% (w/v) Ficoll (Pfizer, Inc., New York, NY) in the resuspension buffer overlaid with 4% Ficoll (as described by Kelley et al., 1983) prepared in 25 mM HEPES-Tris, pH 7.4, containing 1 mM EDTA and 275 mM sucrose. Ficoll gradient tubes were spun at 90,000*g* for 6 to 8 h. The material at the density gradient interfaces was collected, washed, and resuspended in 25 mM HEPES-Tris, pH 7.4, containing 275 mM sucrose. The suspension from this run was resuspended in 25 mM HEPES-Tris buffer containing 150 mM KCl, pH 7.4 (E buffer) with a 25-gauge syringe needle. All of the operations were carried out at 4°C.

BBMVs were prepared according to the method described by Nakamura et al. (2002) with minor modifications. Human term placentas from uncomplicated pregnancies were obtained within 15 min after vaginal or cesarean delivery and placed in 0.9% NaCl. After removal of the cord, amniochorion, and decidua, placental tissue was cut from the maternal side and washed in 250 mM mannitol, 10 mM HEPES-Tris at pH 7.4 (MHT buffer). The mince was stirred for 1 h to loosen the microvilli and filtered through two layers of woven cotton gauze. A sample of this starting mince was taken for enzyme analysis. The filtrate was centrifuged at 800*g* for 10 min. The pellet

was discarded, and $MgCl_2$ was added to the supernatant to a final concentration of 10 mM. After 10 min, with occasional stirring, the supernatant was centrifuged at 10,500*g* for 10 min. The pellet was discarded, and the supernatant was centrifuged at 20,000*g* for 20 min. The pellet from this run was suspended in E buffer with a 25-gauge syringe needle. All of the subsequent procedures were performed at 4°C. BLMVs and BBMVs were quickly frozen and stored at −80°C and used within a month.

Tissue homogenate was prepared by the method previously described by Kelley et al. (1983). Approximately 3 g of whole villous tissue was homogenized in 10 ml of buffer E using a Waring blender (PHYSCOTRON Micro Teq.; Nichion Co., Chiba, Japan) for 2.25 min and further with a homogenizer for eight strokes. The material was filtered through six layers of gauze.

Binding activity of [^{3}H]dihydroalprenolol as a marker of the basal membrane and alkaline phosphatase (ALP) activity as a marker of the microvillous membrane was assayed as reported by Kelley et al. (1983) and Bessey et al. (1946), respectively. The dihydroalprenolol binding of BLMVs was 25.2-fold higher than that of the homogenate, whereas the ALP activity was only 3.07-fold higher. On the other hand, the dihydroalprenolol binding of BBMVs was only 1.07-fold higher than that of the homogenate, whereas the ALP activity was 18.3-fold higher. The amount of protein in the sample was measured by the method of Lowry et al. (1951).

RT-PCR Analysis of OCTs mRNA in Human Placenta and BeWo Cells. The total RNAs of BeWo cells and human placenta were extracted with an RNeasy mini kit (QIAGEN GmbH, Hilden, Germany). Human liver total RNA was purchased from Cell Applications, Inc. (San Diego, CA), and human kidney total RNA was purchased form Stratagene (La Jolla, CA). First-strand cDNA was synthesized from total RNA (50 μg), using random primer and SuperScript II reverse transcriptase (Invitrogen, Carlsbad, CA). PCR was performed with a T-Gradient Thermoblock (Biometra, Göttingen, Germany) using KOD-plus-polymerase (Toyobo Engineering) and primers specific for each family member. Table 1 shows the primer sets used in RT-PCR and the accession number of each transporter.

Western Blotting. HEK293/OCT3 cells, BLMVs, and BBMVs were collected and suspended in lysis buffer containing 100 mM Tris-HCl, pH 7.6, 150 mM NaCl, 1 mM $CaCl_2$, 1% Triton X-100, 0.1% SDS, 0.1% Nonidet P-40, 1 mM phenylmethylsulfonyl fluoride, 0.01 mg/ml leupeptin, 0.01 mg/ml aprotinin, and 1 mM sodium vanadate and incubated for 30 to 45 min at 4°C. After incubation, the suspension was centrifuged at 15,000*g* for 15 min at 4°C. SDS-polyacrylamide gel electrophoresis was performed according to the method of Laemmli (1970). The proteins were transferred electrophoretically onto a 0.2-μm pore size Clear Blot Membrane-P (Atto Corporation, Tokyo, Japan). Blots were blocked overnight at 4°C with 5% nonfat powdered milk in PBS (−). OCT3 (C-14) was used as the primary antibody for OCT3, and horseradish peroxidase anti-goat IgG (Valeant Pharmaceuticals) was used as the secondary antibody. Detection was done with enhanced chemiluminescence reagents (GE Healthcare, Little Chalfont, Buckinghamshire, UK) according to the instructions of the manufacturer.

Uptake Experiment into HEK/OCT3 Cells. HEK/OCT3 cells were seeded at 5 × 10^4 cells/well on 96-well plates (NUNC A/S, Roskilde, Denmark) and grown for 2 days until used for the uptake study.

After reaching confluence, cells were washed twice with uptake buffer (125 mM NaCl, 4.8 mM KCl, 5.6 mM D-glucose, 1.2 mM KH_2PO_4, 1.2 mM $MgSO_4$, and 25 mM HEPES, pH 7.4) before the study. Uptake was initiated by adding 100 μl of uptake buffer containing unlabeled MPP^+ and 10 nM [^{3}H]MPP^+. For the Na^+ dependence study, NaCl was replaced with LiCl, mannitol, or sodium gluconate. After incubation at 37°C for an appropriate time, uptake was terminated by aspiration of the buffer followed by two washes with 1 ml of ice-cold uptake buffer. Cells were then dissolved in 150 μl of 1 N NaOH, and the solution was neutralized with 150 μl of 1 N HCl. Scintillation cocktail (Clear-sol I; Nacalai Tesque, Kyoto, Japan) was added, and the radioactivity of [^{3}H]MPP^+ was determined with a liquid scintillation counter (LS6500; Beckman Coulter, Fullerton, CA). The amount of protein in the cells was measured by the method of Lowry et al. (1951).

Measurement of Uptake into BLMVs and BBMVs. The uptake of [^{3}H]MPP^+ into membrane vesicles was measured by using a rapid filtration technique (Russel et al., 1988). Uptake was initiated by the addition of 90 μl of incubation buffer to 10 μl of BLMV suspension containing 40 to 50 μg of protein. The incubation buffer consisted, in general, of unlabeled MPP^+, 25 mM HEPES-Tris, pH 7.4, 150 mM NaCl, and [^{3}H]MPP^+ (0.08 μCi/point).

At the designated time, uptake was terminated by adding 1 ml of ice-cold stop buffer followed immediately by filtration (HAWP 0.45 μm; Millipore Corporation, Billerica, MA). The filter was washed twice with 4 ml of ice-cold stop buffer. In general, stop buffer contained 10 mM sucrose in incubation buffer. Nonspecific binding was determined by adding 1 ml of ice-cold stop solution and 90 μl of ice-cold incubation buffer to the ice-cold BLMV suspension followed by the same treatment as in the uptake experiments.

To assay radiolabeled compounds, filters were placed in counting vials and mixed with 4 ml of scintillation fluid, Clear-sol I. Radioactivity was measured with a liquid scintillation counter (LS6500).

Data Analysis. The [^{3}H]MPP^+ uptake into HEK/OCT3 cells is expressed as the cell-to-medium ratio calculated from the intracellular uptake per milligram of protein (disintegrations per minute per milligram of protein) of the cells relative to the initial drug concentration (disintegrations per minute per microliter).

As for the uptake into membrane vesicles, obtained radioactivity was normalized with respect to the protein amount of vesicles. Values were determined by subtracting nonspecific binding from total uptake (in the investigation of osmolarity effects as well), and data are presented as the vesicle-to-medium ratio (microliters per milligram of protein).

To determine the kinetic parameters, K_t, J_{max}, and k_d, the following Michaelis-Menten equation was fitted to the data using the nonlinear least-squares regression analysis program MULTI (Yamaoka et al., 1981): $J = J_{max} \times S/(K_t + S) + k_d \times S$, where J and S represent the transport rate and concentration of substrate, respectively. J_{max} (nanomoles per milligram of protein per 30 s), K_t (millimolar), and k_d (microliters per milligram of protein per 30 s) represent the maximum uptake rate for a carrier-mediated process, the Michaelis constant, and the rate constant for the nonsaturable component, respectively.

TABLE 1
Oligonucleotides used for RT-PCR
Open reading frame positions of OCT1, 2, and 3 are 1–1665, 1–1668, and 1–1671, respectively.

Family Member		Sequence	Position	Accession No.
OCT1	Forward	5′-ACTCCGCTCTGGTCGAAATC-3′	1142→1161	X98332
	Reverse	5′-CGACATCGCCGCAAAACATC-3′	1670←1689	
OCT2	Forward	5′-ACTCTGCCCTGGTTGAATTC-3′	1145→1164	X98333
	Reverse	5′-GCAACGGTCTCTCTTCTTAG-3′	1665←1684	
OCT3	Forward	5′-CAGAGATCACTGTTACAGAT-3′	971→990	AJ001417
	Reverse	5′-GATAGCTCCTTCTTTCTGTC-3′	1685←1704	

Comparisons between two and among more than three groups were performed with the unpaired Student's t test and with nonrepeated analysis of variance (ANOVA) followed by Dunnett's test, respectively. The Spearman rank correlation test was used to determine the degree of association between the inhibitory effects on MPP^+ uptake into HEK/OCT3 cells and BLMVs. A P value of less than 0.05 was considered statistically significant.

Results

Expression of OCT mRNAs in Human Placenta and BeWo Cells. The expression of OCTs in human placenta and BeWo cells was examined by RT-PCR analysis. Total RNAs from human liver and kidney were used as positive controls for OCT1 and OCT2 and 3, respectively. In placenta, only OCT3 and the positive control were detected (Fig. 1). The PCR product was confirmed to be in accord with the sequence of human OCT3. With regard to BeWo cells, no band was detected, suggesting that OCTs are not expressed in these cells.

Expression of OCT3 Protein in HEK/OCT3 Cells and Human Placenta. The expression of OCT3 was examined by Western blotting analysis of HEK/OCT3 cells and mock cells (HEK293 cells transfected with vector alone). As expected, a band of 70 kDa was detected only in HEK/OCT3 cells (Fig. 2A).

The expression of OCT3 on human placental trophoblast membrane was also examined by Western blotting analysis using BLMVs and BBMVs prepared from human placenta. The band corresponding to OCT3 was detected in BLMVs at about 70 kDa, as well as in HEK/OCT3 cells, but not in BBMVs (Fig. 2B).

Time Course of the Uptake of MPP^+. The uptake of 1 μM MPP^+ into HEK293/OCT3 cells was significantly higher than that into mock cells (Fig. 3). This uptake was linear for at least 2 min and was attenuated at 4°C. In the following experiments, the initial uptake rate was determined at 30 s.

Effects of Extracellular Ion Composition on the Uptake of MPP^+. The effects of Na^+ and Cl^- on the uptake of MPP^+ were examined by isoosmotic replacement of NaCl (Na^+, +; Cl^-, +) with mannitol (Na^+, −; Cl^-, −), sodium gluconate (Na^+, +; Cl^-, −), and LiCl (Na^+, −; Cl^-, +) in the uptake buffer. As shown in Fig. 4, the uptake of MPP^+ was not affected by any replacement of NaCl, suggesting that OCT3-mediated uptake of MPP^+ is independent of both Na^+ and Cl^-.

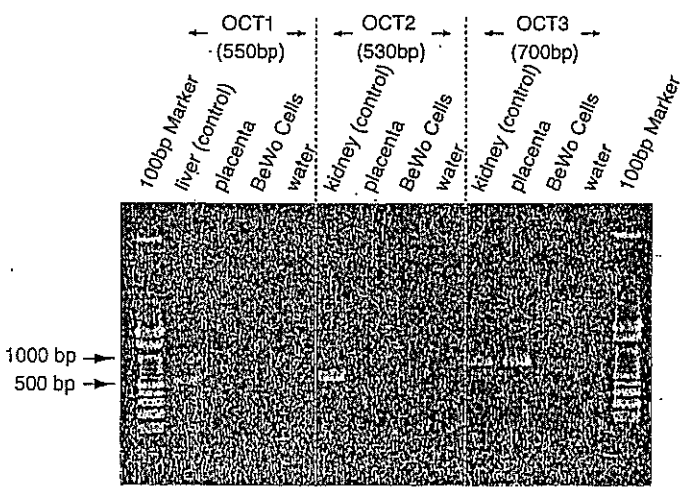

Fig. 1. RT-PCR analysis of the distribution of OCT mRNAs in the human placenta and BeWo cells. Total RNAs from the placenta, liver, kidney, and BeWo cells were reverse-transcribed and used for PCR amplification with oligonucleotide primers specific for OCT1, 2, and 3.

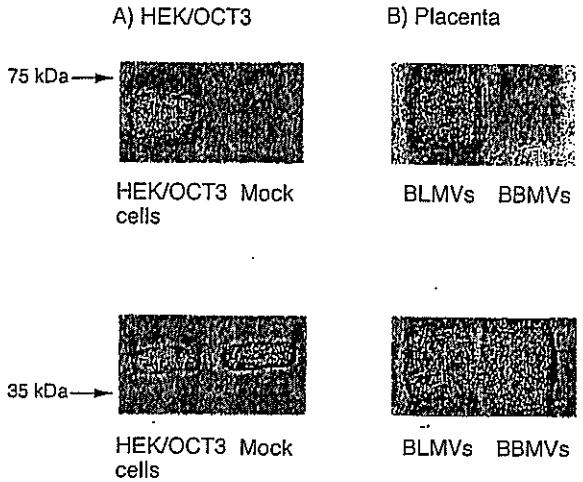

Fig. 2. Western blotting analysis of OCT3 in HEK/OCT3 cells and human placenta. Ten micrograms each of HEK/OCT3 cells and mock (A) and 50 μg each of BLMVs and BBMVs (B) were resolved by SDS-polyacrylamide gel electrophoresis with a 10% polyacrylamide gel and transferred onto Clear Blot Membrane-P. Immunoblots were performed with OCT3-C-14 and anti-β-actin mouse monoclonal antibody and developed with the enhanced chemiluminescence detection reagent. OCT3 and β-actin were detected at 70 and 40 kDa, respectively.

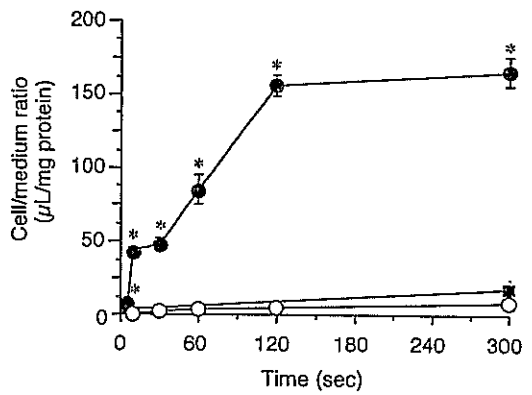

Fig. 3. Time course of OCT3-mediated uptake of 1 μM MPP^+. HEK/OCT3 cells were incubated at 37 (closed circle) and 4°C (closed triangle). HEK293 cells transfected with vector alone (open circle) were incubated at 37°C. Each point represents the mean ± S.E.M. of four determinations. *, $P < 0.05$ versus control (Student's t test).

Concentration-Dependent Uptake of MPP^+. The OCT3-mediated uptake was saturable with a Michaelis constant (K_t) of 82.5 μM (59.7–113.8) [mean (mean − S.D. − mean + S.D.)] and a maximal uptake velocity (J_{max}) of 2538 ± 567.4 pmol/mg protein/30 s (mean ± S.D.) (Fig. 5) obtained from three separate experiments.

Inhibitory Effects of Various Cationic Compounds on the OCT3-Mediated Uptake of MPP^+. The OCT3-mediated uptake of 10 μM MPP^+ was significantly inhibited by various cationic drugs, such as cimetidine, ranitidine, verapamil, quinine, quinidine, imipramine, trimethoprim, and procainamide, in a concentration-dependent manner (Figs. 6 and 7). In contrast, anionic compounds [p-aminohippuric acid (PAH), captopril, and phenobarbital], a zwitterion (carnitine), and a cationic compound (lamivudine) showed little or no inhibitory effect.

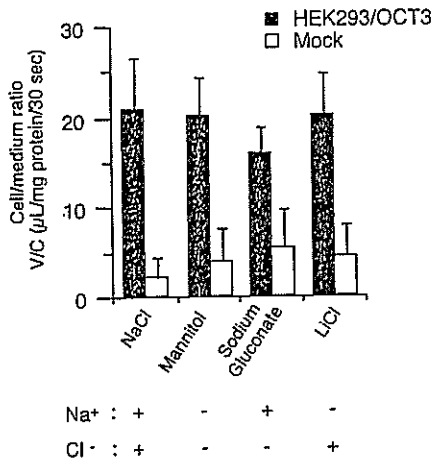

Fig. 4. OCT3-mediated uptake of MPP^+ in the presence or absence of Na^+ or Cl^-. HEK/OCT3 cells were incubated at 37°C for 30 s with 10 μM MPP^+. Uptake buffers of different ionic composition were used: NaCl (Na^+, +; Cl^-, +), mannitol (Na^+, −; Cl^-, −), sodium gluconate (Na^+: +, Cl^-: −), LiCl (Na^+, −; Cl^-, +). Each point represents the mean ± S.E.M. of four determinations.

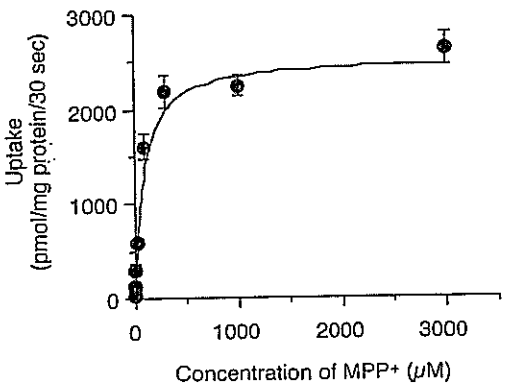

Fig. 5. Concentration-dependent uptake of MPP^+ into HEK/OCT3 cells. Uptake of MPP^+ into HEK/OCT3 cells and mock was measured at concentrations between 1 μM and 3 mM. Data are presented as the OCT3-specific uptake calculated by subtracting the uptake obtained with mock from that obtained with HEK/OCT3. Each point represents the mean ± S.E.M. obtained from three different experiments.

Uptake of Various Cationic Compounds. To search for novel substrates of OCT3, we examined the uptake of 10 μM tetraethylammonium, quinine, theophylline, and ramosetron into HEK/OCT3 cells. No OCT3-mediated uptake of these compounds was observed (data not shown).

Uptake of MPP^+ into BLMVs. The vesicle-to-medium ratio of MPP^+ in BLMVs was linear for at least 30 s (Fig. 8). The vesicle-to-medium ratio at 10 min was reduced with increasing extracellular osmolarity, suggesting that MPP^+ was not only bound to the vesicles but also was taken up into the vesicles.

This uptake was significantly attenuated by replacing extravesicular NaCl with KCl and was potentiated by the addition of valinomycin, a potassium ionophore. The uptake of MPP^+ was not affected by the replacement of NaCl with LiCl (Fig. 9). These results suggested that the uptake of MPP^+ into BLMVs is dependent on membrane potential and independent of Na^+.

Concentration-Dependent Uptake of MPP^+ into BLMVs. The uptake of MPP^+ into BLMVs was saturable with a Michaelis constant (K_t) of 51.8 μM [34.9–113.8] (mean [mean − S.D. − mean + S.D.]) and a maximal uptake velocity (J_{max}) of 332 ± 30.8 pmol/mg protein/30 s (mean ± S.D.) (Fig. 10) obtained from three separate experiments.

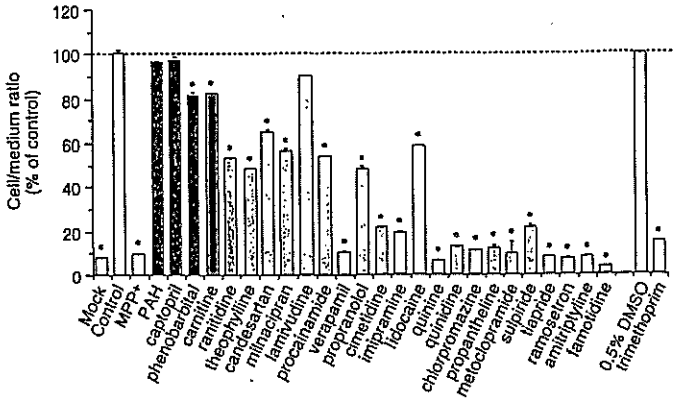

Fig. 6. Inhibitory effects of several drugs on the uptake of MPP^+ into HEK/OCT3 cells. HEK/OCT3 cells were incubated at 37°C for 30 s with 10 μM MPP^+ in the absence or presence of 1 mM various compounds. Results are given as percentage of control uptake measured in the absence of inhibitors. The control and control [+0.5% dimethyl sulfoxide (DMSO)] values were 27.38 and 25.04 μl/mg protein/30 s. Each point represents the mean ± S.E.M. of four determinations. *, $P < 0.05$ versus respective control (ANOVA; Dunnett's test).

Effects of Various Compounds on the Uptake of MPP^+ into BLMVs. We examined the effects of various compounds of the uptake of MPP^+ into BLMVs. We selected noninhibitors (PAH, captopril, and lamivudin), modest inhibitors (carnitine and procainamide), and strong inhibitors (cimetidine, imipramine, quinidine, verapamil, and quinine) of OCT3-mediated uptake. As shown in Fig. 11, PAH and procainamide showed little or no inhibitory effect, whereas quinine, quinidine, imipramine, and verapamil inhibited the uptake of MPP^+ into BLMVs. The rank order of the inhibitory effects of MPP^+ uptake into HEK/OCT3 cells was highly correlated with that in BLMVs ($r^2 = 0.688$, $P < 0.05$; Fig. 12).

Discussion

To investigate the placental transport mechanism of cationic compounds, we focused on OCTs in this study. Because the only OCT detected in human placenta by RT-PCR analysis was OCT3, this molecule is expected to play an important role in the transport of cationic compounds across the human placenta.

hOCT1 and hOCT2 are predominantly expressed in the liver and kidney, respectively (Gorboulev et al., 1997). Unlike OCT1 and OCT2, OCT3 is widely expressed (Kekuda et al., 1998; Verhaagh et al., 1999). The OCT3 mRNA level in the placenta is particularly high, being 2.5 and 5 times that in the liver and kidney, respectively. OCT3 is considered to be one of the most abundantly expressed transporters in the placenta (Leazer and Klaassen, 2003). Our results are consistent with that finding and underscore the key role of OCT3 in the transport of cationic compounds in the placenta.

We also investigated OCTs in a human choriocarcinoma trophoblast cell line, BeWo cells, and found no expression of OCTs. This finding is in accordance with the results of Wu et al. (2000). Although the BeWo cell line originated from placenta, it has the characteristics of cytotrophoblast cells and is functionally and morphologically distinct from normal syncytiotrophoblast cells (Ugele and Simon, 1999). Thus, it is not surprising that OCT3 is not expressed in BeWo cells.

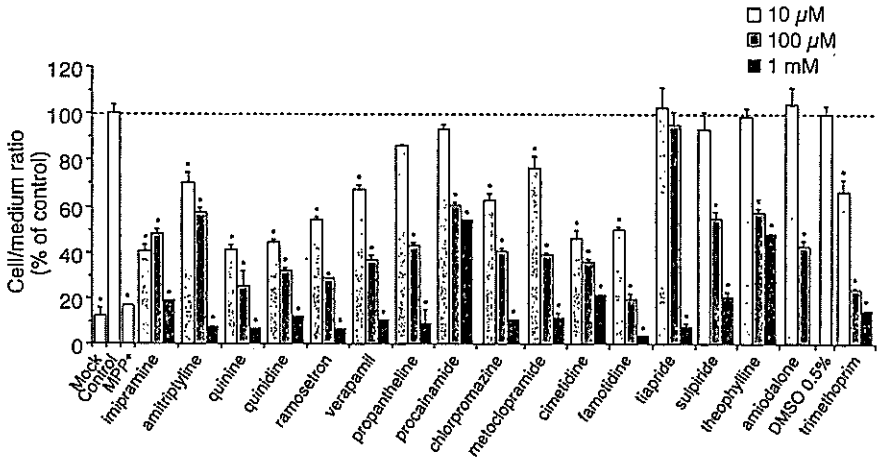

Fig. 7. Inhibitory effects of several drugs on the uptake of MPP^+ into HEK/OCT3 cells. HEK/OCT3 cells were incubated at 37°C for 30 s with 10 μM MPP^+, in the absence or presence of 10 or 100 μM or 1 mM inhibitors. Results are given as percentage of control uptake measured in the absence of inhibitors. The control and control [+0.5% dimethyl sulfoxide (DMSO)] values were 29.97 μl/mg protein/30 s and 28.54 μl/mg protein/30 s. Each point represents the mean ± S.E.M. of four determinations. *, $P < 0.05$ versus respective control (ANOVA; Dunnett's test).

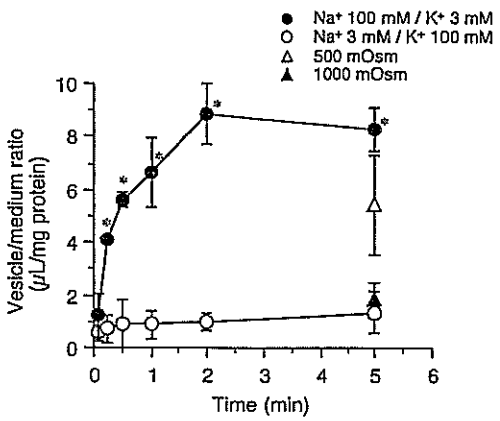

Fig. 8. Influence of Na^+ on the uptake of MPP^+ into BLMVs. Uptake was initiated by the addition of 10 μM MPP^+ in the presence of Na^+ 100 mM/K^+ 3 mM (closed circle) or Na^+ 3 mM/K^+ 100 mM (open circle). Each point represents the mean ± S.E.M. of three determinations. *, $P < 0.05$ versus control (Student's t test).

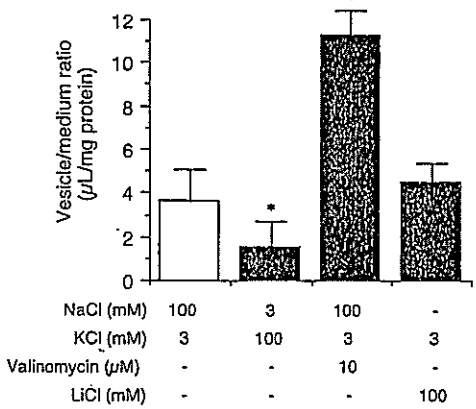

Fig. 9. Influence of membrane potential on the uptake of MPP^+ into BLMVs. Uptake was initiated by the addition of 10 μM MPP^+. Ionic composition of uptake buffers is shown below the figure. Each point represents the mean ± S.E.M. of three determinations. *, $P < 0.05$ versus control (ANOVA; Dunnett's test).

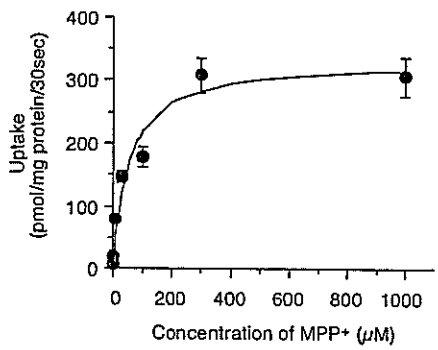

Fig. 10. Concentration-dependent uptake of MPP^+ into BLMVs. Uptake of MPP^+ into BLMVs was measured at concentrations between 1 μM and 1 mM. Uptake was initiated by the addition of 10 μM MPP^+ in the presence of Na^+ 100 mM/K^+ 3 mM. Each point represents the mean ± S.E.M. obtained from three different experiments.

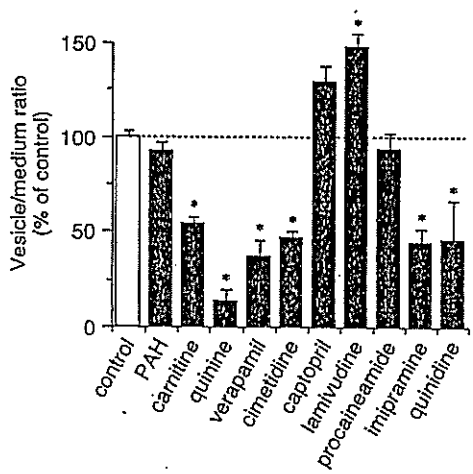

Fig. 11. Inhibitory effects of several drugs on the uptake of 10 μM MPP^+ into BLMVs. BLMVs were incubated at 37°C for 30 s with 10 μM MPP^+, in the absence or presence of 1 mM various compounds. Results are given as percentage of control uptake measured in the absence of inhibitors. The control values were 4.02 μl/mg protein/30 s. Each point represents the mean ± S.E.M. of three determinations. *, $P < 0.05$ versus control (ANOVA; Dunnett's test).

Western blotting demonstrated predominant expression of OCT3 in HEK/OCT3 cells. It was detected as a band of 70 kDa, which is larger than expected from the amino acid sequence (62 kDa) (Fig. 2). Because both mouse and rat OCT3 have four to five N-glycosylation sites (Burckhardt and Wolff, 2000) and hOCT3 shows 90% homology to them, the difference in size is likely to be attributable to glycosylation. Indeed, the size of the bands of OCT3 from both BLMVs and HEK/OCT3 cells was 70 kDa. The established HEK/OCT3 cells transported MPP^+ with a K_t value of 69 μM (Fig. 5), which is in good agreement with the values reported for human retinal pigment epithelial cells (47 μM; Wu et al., 2000) and HEK293 (104 μM; Martel et al., 2001).

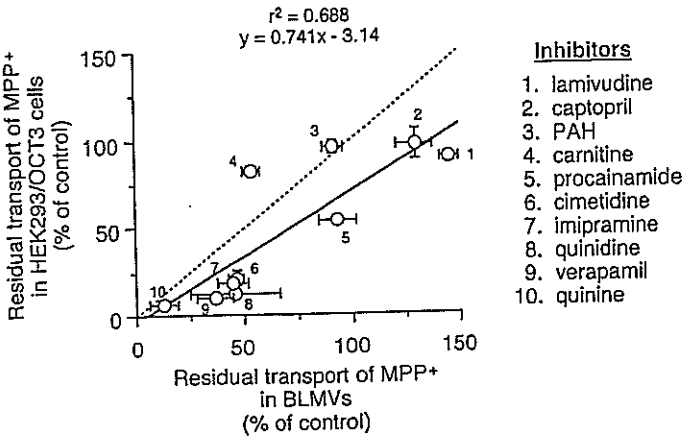

Fig. 12. Comparison of inhibitory effects on MPP+ uptake between HEK/OCT3 cells and BLMVs. The solid line shows the linear regression and the dashed line shows the 1:1 line. The concentration of each inhibitor was 1 mM. Each point represents the mean ± S.E.M. of three (BLMVs) or four (HEK/OCT3 cells) determinations.

The uptake of MPP^+, a typical substrate of OCT3, into HEK/OCT3 cells was inhibited by cationic compounds, such as cimetidine, verapamil, quinine, quinidine, ramosetron, and trimethoprim, in a concentration-dependent manner. In contrast, anionic compounds, including PAH, captopril, and phenobarbital, and a zwitterion, carnitine, showed little or no inhibitory effect (Figs. 6 and 7). In addition to well known inhibitors of OCT3, such as cimetidine, imipramine, and quinine (Gründemann et al., 1998; Wu et al., 2000), we have identified a variety of cationic drugs that inhibit OCT3. Interestingly, a cationic compound, lamivudine, did not inhibit OCT3 function, suggesting that cationic character alone is not sufficient for recognition by OCT3. Among therapeutic drugs, only cimetidine is known to be a substrate of OCT3 (Gründemann et al., 1999). Because various cationic drugs were found to inhibit OCT3, some of them might be substrates of OCT3.

To search for novel substrates of OCT3, we also examined the uptake of tetraethylammonium, quinine, theophylline, and ramosetron into HEK/OCT3 cells. Although tetraethylammonium is a typical substrate of OCT1 and 2 as well as MPP^+, none of the above-mentioned drugs was a substrate for OCT3. Our finding in the case of tetraethylammonium is consistent with previous reports that the affinity of tetraethylammonium for mouse and rat OCT3 is approximately 10-fold weaker than that for OCT1 and 2 (Kekuda et al., 1998; Wu et al., 2000) and that hOCT3 does not interact with tetraethylammonium (Gründemann et al., 1999). In contrast, OCT3 has high affinity for monoamines (Gründemann et al., 1998). Overall, OCT3 seems to have a substrate specificity distinct from those of OCT1 and 2.

Western blot analysis of BLMVs and BBMVs showed that OCT3 is predominantly expressed on the basolateral membrane of trophoblast cells (Fig. 2). Recently, it has been reported that accumulation of MPP^+ in the embryo was reduced in OCT3-knockout pregnant mice, although MPP^+ concentrations in the placenta and amniotic fluid were comparable (Zwart et al., 2001), suggesting that OCT3 mediates the transport of MPP^+ from the placenta to the fetus but not from the maternal circulation to the placenta. This finding is consistent with our results that OCT3 is expressed on the basolateral membrane of trophoblast cells. Although various transporters, such as organic cation/proton antiporter, norepinephrine transporter, and serotonin transporter, were shown to be localized at the microvillous membrane of placental trophoblast cells (Ganapathy et al., 2000), nothing was known about the expression of transporters for cationic compounds on the basolateral membrane of trophoblast cells. Herein, we have demonstrated for the first time the expression and function of OCT3 on the basal membrane, where it presumably plays a role in the excretion of metabolic waste products or xenobiotics from the fetus. With regard to the transport direction, OCT3 has been considered to transport cationic compounds bidirectionally in a concentration-dependent manner (Kekuda et al., 1998). OCT3 may transport the maternally administered cationic compounds from the placenta to the fetal side and transport oppositely the cationic compounds whose level is higher in the fetal blood.

We compared quantitatively the transport properties of cationic compounds in human placental membrane vesicles with those of HEK/OCT3 cells. The uptake of MPP^+ into BLMVs was membrane potential-sensitive and Na^+-independent (Fig. 9). The K_m values of MPP^+ uptake into BLMVs and HEK/OCT3 cells were similar (39 and 70 μM, respectively). Moreover, the inhibitory effects of various compounds on the uptake of MPP^+ into BLMVs were highly correlated with those on uptake into HEK/OCT3 cells (Fig. 12). Because we did not examine detailed mechanism for the inhibition by drugs, we cannot exclude the possibility that they inhibited OCT3 in a noncompetitive manner by a nonspecific mechanism, such as membrane depolarization and so on. Although the inhibitory mechanism by these compounds remains to be further investigated, the inhibitory nature is unlikely to significantly affect the conclusion that OCT3 plays an important role in the placental transport of cationic compounds.

In summary, we have identified the expression of OCT3 on the basal membranes of trophoblast cells. Because the properties of MPP^+ uptake into BLMVs are similar to those in HEK/OCT3 cells, OCT3 is likely to be predominantly responsible for the transport of cationic compounds across the basolateral membranes of trophoblast cells.

References

Bessey OA, Lowry OH, and Brock MJ (1946) A method of the rapid determination of alkaline phosphatase with five cubic millimeters of serum. *J Biol Chem* 28:321–329.

Burckhardt G and Wolff NA (2000) Structure of renal organic anion and cation transporters. *Am J Physiol* 278:F853–F866.

Dresser MJ, Leabman MK, and Giacomini KM (2000) Transporters involved in the elimination of drugs in the kidney: organic anion transporters and organic cation transporters. *J Pharm Sci* 90:397–421.

Ganapathy V, Prasad PD, Ganapathy ME, and Leibach FH (2000) Placental transporters relevant to drug distribution across the maternal-fetal interface. *J Pharmacol Exp Ther* 294:413–420.

Gorboulev V, Ulzheimer JC, Akhoundova A, Ulzheimer-Teuber I, Karbach U, Quester S, Baumann C, Lang F, Busch AE, and Koepsell H (1997) Cloning and characterization of two human polyspecific organic cation transporters. *DNA Cell Biol* 16:871–881.

Gründemann D, Gorboulev V, Gambaryan S, Veyhl M, and Koepsell H (1994) Drug excretion mediated by a new prototype polyspecific transporter. *Nature (Lond)* 372:549–552.

Gründemann D, Liebich G, Kiefer N, Koster S, and Schomig E (1999) Selective substrates for non-neuronal monoamine transporters. *Mol Pharmacol* 56:1–10.

Gründemann D, Schechinger B, Rappold GA, and Schomig E (1998) Molecular identification of the corticosterone-sensitive extraneuronal catecholamine transporter. *Nat Neurosci* 1:349–351.

Hohage H and Gerhardt U (2000) Inorganic anions and the renal organic cation transport system. *Life Sci* 66:1–9.

Inuyama M, Ushigome F, Emoto A, Koyabu N, Satoh S, Tsukimori K, Nakano H, Ohtani H, and Sawada Y (2002) Characteristics of L-lactic acid transport in basal membrane vesicles of human placental syncytiotrophoblast. *Am J Physiol* 283: C822–C830.

Kamisako T, Gabazza EC, Ishihara T, and Adachi Y (1999) Molecular aspects of

organic compound transport across the plasma membrane of hepatocytes. *J Gastroenterol Hepatol* 14:405–412.
Karbach U, Kricke J, Meyer-Wentrup F, Gorboulev V, Volk C, Loffing-Cueni D, Kaissling B, Bachmann S, and Koespell H (2000) Localization of organic cation transporters OCT1 and OCT2 in rat kidney. *Am J Physiol* 279:F679–F687.
Kekuda R, Prasad PD, Wu X, Wang H, Fei YJ, Leibach FH, and Ganapathy V (1998) Cloning and functional characterization of a potential-sensitive, polyspecific organic cation transporter (OCT3) most abundantly expressed in placenta. *J Biol Chem* 273:15971–15979.
Kelley LK, Smith CH, and King BF (1983) Isolation and partial characterization of the basal cell membrane of human placental trophoblast. *Biochim Biophys Acta* 734:91–98.
Koepsell H (1998) Organic cation transporters in intestine, kidney, liver and brain. *Annu Rev Physiol* 60:243–266.
Laemmli UK (1970) Cleavage of structural proteins during the assembly of the head of bacteriophage T4. *Nature (Lond)* 227:680–685.
Lahjouji K, Elimrani I, Lafond J, Leduc L, Qureshi IA, and Mitchell GA (2004) L-Carnitine transport in human placental brush-border membranes is mediated by the sodium-dependent organic cation transporter OCTN2. *Am J Physiol* 287: C263–C269.
Leazer TM and Klaassen CD (2003) The presence of xenobiotic transporters in the rat placenta. *Drug Metab Dispos* 31:153–167.
Lowry OH, Rosebrough NJ, Farr AL, and Randall RJ (1951) Protein measurement with the Folin phenol reagent. *J Biol Chem* 193:265–275.
Martel F, Keating E, Calhau C, Gründemann D, Schömig E, and Azevedo I (2001) Regulation of human extraneuronal monoamine transporter (hEMT) expressed in HEK293 cells by intracellular second messenger systems. *Naunyn-Schmiedeberg's Arch Pharmacol* 364:487–495.
Meyer-Wentrup F, Karbach U, Gorboulev V, Arndt P, and Koespell H (1998) Membrane localization of the electrogenic cation transporter rOCT1 in rat liver. *Biochem Biophys Res Commun* 248:673–678.
Nakamura H, Ushigome F, Koyabu N, Satoh S, Tsukimori K, Nakano H, Ohtani H, and Sawada Y (2002) Proton gradient-dependent transport of valproic acid in human placental brush-border membrane vesicles. *Pharm Res* 19:154–161.
Okuda M, Saito H, Urakami Y, Takano M, and Inui K (1996) cDNA cloning and functional expression of a novel rat kidney organic cation transporter, OCT2. *Biochem Biophys Res Commun* 224:500–507.
Russel FG, van der Linden PE, Vermeulen WG, Heijn M, van Os CH, and van Ginneken CA (1988) Na^+ and H^+ gradient-dependent transport of *p*-aminohippurate in membrane vesicles from dog kidney cortex. *Biochem Pharmacol* 37:2639–2649.
Schweifer N and Barlow DP (1996) The Lx1 gene maps to mouse chromosome 17 and codes for a protein that is homologous to glucose and polyspecific transmembrane transporters. *Mamm Genome* 7:735–740.
Sugawara-Yokoo M, Urakami Y, Koyama H, Fujikura K, Masuda S, Saito H, Naruse T, Inui K, and Takata K (2000) Differential localization of organic cation transporters rOCT1 and rOCT2 in the basolateral membrane of rat kidney proximal tubules. *Histochem Cell Biol* 114:175–180.
Suzuki H and Sugiyama Y (2000) Transport of drugs across the hepatic sinusoidal membrane: sinusoidal drug influx and efflux in the liver. *Semin Liver Dis* 20:251–263.
Tamai I, Yabuuchi H, Nezu J, Sai Y, Oku A, Shimane M, and Tsuji A (1997) Cloning and characterization of a novel human pH-dependent organic cation transporter, OCTN1. *FEBS Lett* 419:107–111.
Ugele B and Simon S (1999) Uptake of dehydroepiandrosterone-3-sulfate by isolated trophoblasts from human term placenta, JEG-3, BeWo, Jar, BHK cells and BHK cells transfected with human sterylsulfatase-cDNA. *J Steroid Biochem Mol Biol* 71:203–211.
Ushigome F, Koyabu N, Satoh S, Tsukimori K, Nakano H, Nakamura T, Uchiumi T, Kuwano M, Ohtani H, and Sawada Y (2003) Kinetic analysis of P-glycoprotein-mediated transport by using normal human placental brush-border membrane vesicles. *Pharm Res* 20:38–44.
Verhaagh S, Schweifer N, Barlow DP, and Zwart R (1999) Cloning of the mouse and human solute carrier 22a3 (Slc22a3/SLC22A3) identifies a conserved cluster of three organic cation transporters on mouse chromosome 17 and human 6q26–q27. *Genomics* 55:209–218.
Wu X, Huang W, Ganapathy ME, Wang H, Kekuda R, Conway SJ, Leibach FH, and Ganapathy V (2000) Structure, function and regional distribution of the organic cation transporter OCT3 in the kidney. *Am J Physiol* 279:F449–F458.
Yamaoka K, Tanigawara Y, Nakagawa T, and Uno T (1981) A pharmacokinetic analysis program (MULTI) for microcomputer. *J Pharmacobio-Dyn* 4:879–881.
Zhang L, Gorset W, Dresser MJ, and Giacomini KM (1999) The interaction of *n*-tetraalkylammonium compounds with a human organic cation transporter, hOCT1. *J Pharmacol Exp Ther* 288:1192–1198.
Zwart R, Verhaagh S, Buitelaar M, Popp-Snijders C, and Barlow DP (2001) Impaired activity of the extraneuronal monoamine transporter system known as uptake-2 in *Orct3/Slc22a3*-deficient mice. *Mol Cell Biol* 21:4188–4196.

Address correspondence to: Dr. Yasufumi Sawada, Graduate School of Pharmaceutical Sciences, Kyushu University, 3-1-1 Maidashi, Higashi-ku, Fukuoka 812-8582, Japan. E-mail: sawada@phar.kyushu-u.ac.jp

総　説

がん分子標的治療開発に関する基盤研究

—ベットサイドへの貢献を目指して—

久留米大学先端癌治療研究センター分子外科部門
癌分子標的治療研究部門（久留米大学 COE）

桑野信彦※・藤井輝彦

我々の部門では，分子外科のスタッフを中心にアジアからのポストドク，大学院生と研究生らで仕事を進めている．1カ月に2回の英文論文抄読会と1回の仕事発表会を行っている．約2年経過してがんの分子標的に関する研究の基盤が少しずつ構築されはじめた状況である．特に大切にしているのは久留米から独自性のあるがん研究を発信することであり，がんの診断・治療と予防などに貢献できる仕事を発展させたいと祈念している．学内の各教室の協力に加えて九州大学・院医・医化学教室の小野眞弓先生（久留米大学・客員教授予定）や産業医科大学・医・分子生物学教室の河野公俊先生（久留米大学・客員教授予定）らの研究グループ，さらに大鵬薬品飯能研究センター長の山田雄次先生（久留米大学・客員教授予定）らの研究グループと人的交流や共同研究を進めている．

研究プロジェクトとしては現在次の2項目について進めている．

Ⅰ．抗がん剤感受性／耐性や効果を制御するがん細胞の分子標的
1．抗がん剤の感受性を制御するABC（ATP結合力セット）トランスポーター[1)-4)]
2．抗がん剤の感受性を制御するYB-1（Y-box結合蛋白-1）[5)6)]
3．分子標的薬剤Gefitinib（イレッサ）の感受性を左右する機序と標的[7)-10)]
4．肝癌におけるインターフェロンαと他剤との併用効果を制御する因子

Ⅱ．がんの分子や転移また生存率／予後に関わる分子標的と血管新生及びマクロファージ
1．膵癌，乳癌，肝癌におけるCap43/NDRG1の機能と臨床的意義[11)-14)]
2．肝癌におけるIGF（インスリン様増殖因子）シグナルの働きと臨床的意義
3．がんの間質応答の中で炎症性サイトカインで誘導される血管新生とマクロファージ[15)16)]

上記のプロジェクトの中からI-1（I-2の一部を含む）とI-3の2つを選んで簡単に説明したい．

Ⅰ．ABCトランスポーター

1．胆汁排出の一つの鍵をにぎるABCトランスポーター：MRP2/cMOAT/ABCC2

ABCトランスポーター（ATP結合カセットトランスポーター）は現在，約50個近くヒトノゲム上に存在するが，ATP結合部位が2箇所ある膜貫通型糖蛋白質でイオンチャンネル（のう胞性線維症の原因遺伝子なども含む）や生理活性物質や異物の輸送を担うトランスポーターとして働く．我々の身体の多くの臓器に発現しているが，特に血液・脳関門をはじめ血管・臓器関門に発現して我々の体内で異物や毒物などから防御したり生理活性物質の排出や吸収に働いて生体の恒常性を保持するのに重要である（図1A，B）．図1Cに腸肝循環における幾つかのABCトランスポーターの局在と発現を示す．我々は1996年にヒトMRP2/ABCC2をはじめて単離し[1)]，さらに体質

※学長特命教授
M. Kuwano and T. Fujii. Development of anticancer molecular targeting diagnosis and therapeutics strategy from beach to bed.

性黄疸症である Dubin-Johnson（D-J）症候群の原因遺伝子であることを明らかにした[2)3)]．MRP2 の D-J 遺伝子変異のうち Q1382R は成熟型（180～190KDa）を示すが ATP 分解活性がないこと，さらに R768W や K667R の変異は前駆体（160～170KDa）から活性型の成塾型へ変換しないために高ビリルビン血症をひきおこすことを明らかにした（図２）[4)]．さらに MRP2 もまた炎症関連物質であるロイコトリエン C4 だけでなくビンカアルカロイド，カンプトテシンやシスプラチンなどの抗がん剤感受性にも関与することを見出した．

２．YB-1（Y-ボックス結合蛋白-1）とがんにおける P-糖蛋白質の発現

P-糖蛋白質（MDR1）は代表的な ABC トランスポーターであり，抗がん剤だけでなく，抗アレルギー剤，抗生物質，免疫抑制物質，カルシウム拮抗剤，ステロイド，循環器系薬剤，モルヒネ，脳神経薬剤など実に多岐にわたる薬剤を基質とすることが知られている．他方，P-糖蛋白質のが

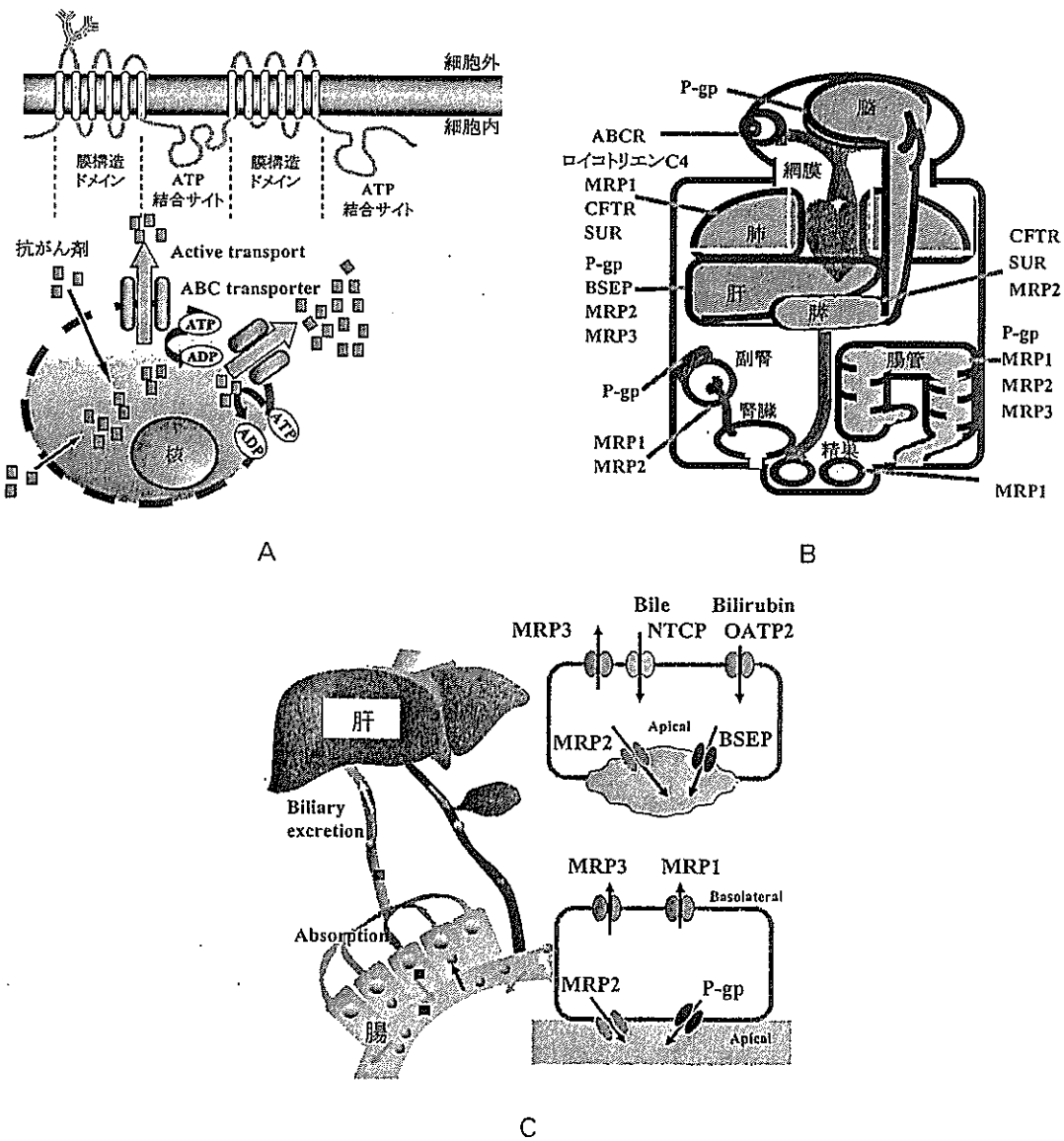

図１　A　ABC トランスポーターの構造と機能．
B　各臓器で異物や生理活性物質の輸送・排泄に関与する ABC トランスポーターの臓器や血液・臓器関門における発現と局在．
C　腸肝における ABC トランスポーターと他のトランスポーターの発現と局在．

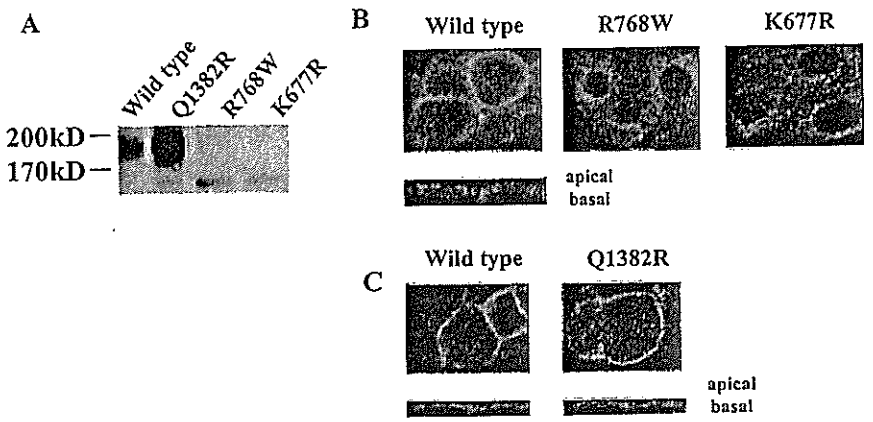

図2　野性型と D-J 変異 Q1382R の MRP2 は 180-190KDa の分子量を示すが，他の D-J 変異 R768W と K677R は 170KDa の前駆体のままである（A）．さらに野性型 MRP2 は細胞膜に局在するが，2 つの D-J 変異型は細胞質に未成熟型として存在する（B）．また野性型と Q138R は apical 側に局在する（C）．

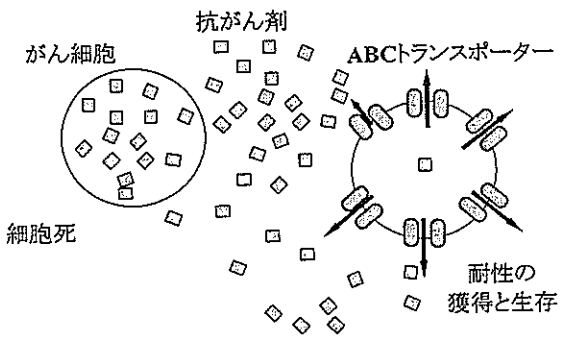

図3　ABC トランスポーターと治療：P-糖蛋白質を代表する ABC トランスポーターが発現すると親和性のある抗がん剤に対して多剤耐性の獲得や感受性を変化させる．

んにおける発現上昇はしばしば抗がん剤治療に対する多剤耐性の獲得を誘導する（図3）．

抗がん剤治療の後に，P-糖蛋白質のがんにおける過剰発現は色々のタイプのがんでしばしば観察される．臨床がんにおいて治療のあとの P-糖蛋白質依存性の多剤耐性の獲得に関与する機序として我々は，MDR1 遺伝子の発現を制御するプロモーター領域の CpG のメチル化の有無が重要であることを白血病と膀胱癌患者で見出した．他方もう一つの機序として図4に示すように細菌からヒトまで保存されているコールドショック・ドメインをもつ原始的な蛋白質である YB-1 の核内局在が P-糖蛋白質の発現上昇に重要な鍵をにぎっていることをヒトがんで観察した．抗がん剤や放射線による DNA 障害によって MDR1 遺伝子発現が誘導されること，そしてその誘導に YB-1 が関与することを河野公俊博士らと共同で 1989 年に発見した[5]．この YB-1 が MDR1 遺伝子の発現誘導とシスプラチンなどの DNA 障害の修復に関与することを観察した（図4）．そこでこの基礎知識をもとにがん患者ではどうかという問いかけを行った．その結果，乳癌をはじめ幾つかの種類のがんで P-糖蛋白質の発現と YB-1 の核内局在が緊密に相関することが見出されている[6]．YB-1 が臨床診断や治療にも有用な分子標的となるか否かが今後の我々の課題である．

Ⅱ．EGF レセプター（EGFR）と Cap43/NDRG1/Drg-1 はがん治療薬開発や悪性病理診断の分子標的？

1．古くて新しい増殖因子レセプターである EGFR ファミリー

がんの悪性形質の獲得に関与する分子を標的にした分子標的薬剤の登場は最近のハイライトである[7]．分子標的薬剤の使用にあたって “proof of principle” を患者で明らかにしていくことが大切であるといわれている．ゲフィチニブ（イレッ

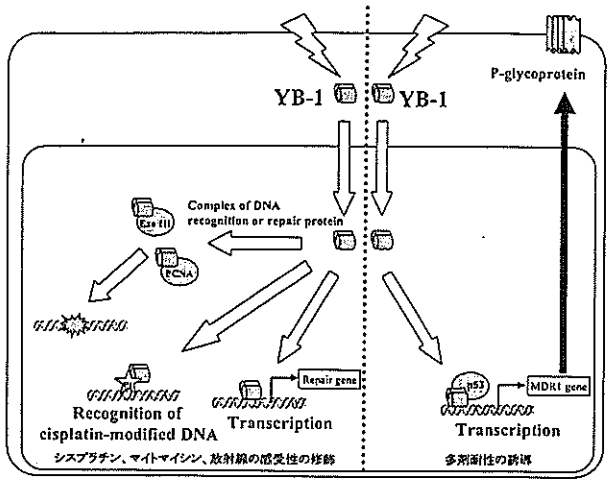

A

癌種	薬剤耐性関連標的分子
卵巣癌	シスプラチン耐性 P-糖蛋白質上昇
乳癌	P-糖蛋白質上昇 抗がん剤耐性
骨肉腫	P-糖蛋白質上昇
滑膜肉腫	P-糖蛋白質上昇
前立腺癌	P-糖蛋白質上昇 アンドロゲン不応答

B

図4　A　YB-1による薬剤感受性の制御は2つの経路が関与する．抗がん剤や放射線照射によってYB-1が核内へ移行しシスプラチンなどのP-糖蛋白質非依存性の耐性とP-糖蛋白質依存性の多剤耐性に関与する我々のモデル．
B　YB-1核内局在とP-糖蛋白質発現中薬剤耐性が有意な相関を示すヒトがん．

サ）やハーセプチンは肺癌や乳癌のEGFRファミリーであるEGFRやHER2を標的としており，久留米大学ではイレッサとハーセプチンの併用に関する基礎研究が進められている[8]．EGFRのチロシンキナーゼ・ドメインの変異の中にゲフィチニブに高感受性である非小細胞肺癌（NSCLC）症例が見出され注目されている．さらに高感受性を示す日本人女性の非小細胞肺癌（腺癌）にEGFRの突然変異の頻度が高いことが報告されている．小野眞弓博士らも世界に先駆け独立に，NSCLCの各々のEGFRシグナルが各細胞の増殖や細胞死とどれだけ緊密に関連しているか否かが肺癌細胞のゲフィチニブ感受性の鍵をにぎっていることを報告している[9]（図5）．現在さらにHER2やHER3のヘテロダイマーの形成の有無が同薬剤の治療効果のもう一つの鍵をにぎるのではないかと考えて研究が進められている[10]．

2．分化能や転移抑制と関連するCap43/NDRG1/Drg-1

Cap43遺伝子はカルシウムで誘導される分子量が43KDaのタンパクであり，Charcott-Marie-Tooth病の原因遺伝子でもある．最近，ノックアウトマウスで神経の脱エミリン化をひきおこしていること[11]や，さらに神経の再生や分化にも深くかかわることが知られている[12]．低酸素，金属イオン，ホルボールエステル，p53，N-mycなどでその発現が著明に修飾されるが，我々は2001年にヒト腎癌から同遺伝子を単離した[13][14]．最近，前立腺癌や乳癌でCap43の発現が予後マーカーとして報告されて以来，Cap43に関する研究が次第に増えはじめている．我々は，Cap43の発現が膵癌，乳癌また肝癌の治療効果の判定マーカーになるのではないかと考えて研究を進めている．現在，丸山祐一郎君（久留米大・外科）らは“何故膵癌は悪性度が高いのか？”“何かいい治療法はないか？”という問いかけのもとに膵癌でのCap43の研究に取組んでおり，Cap43の発現が膵癌の予後や転移能と緊密に関連することを観察している（Maruyama，Aoyagi，Kinoshita，Kuwanoら論文準備中）．

以上，現在進行中の幾つかのプロジェクトについて簡単に記載した．これらの分子標的や基礎研究の中からベットサイドへ役に立つ有用なものを我々の研究部門から一つでも二つでも提示できるように努力をしていきたい．

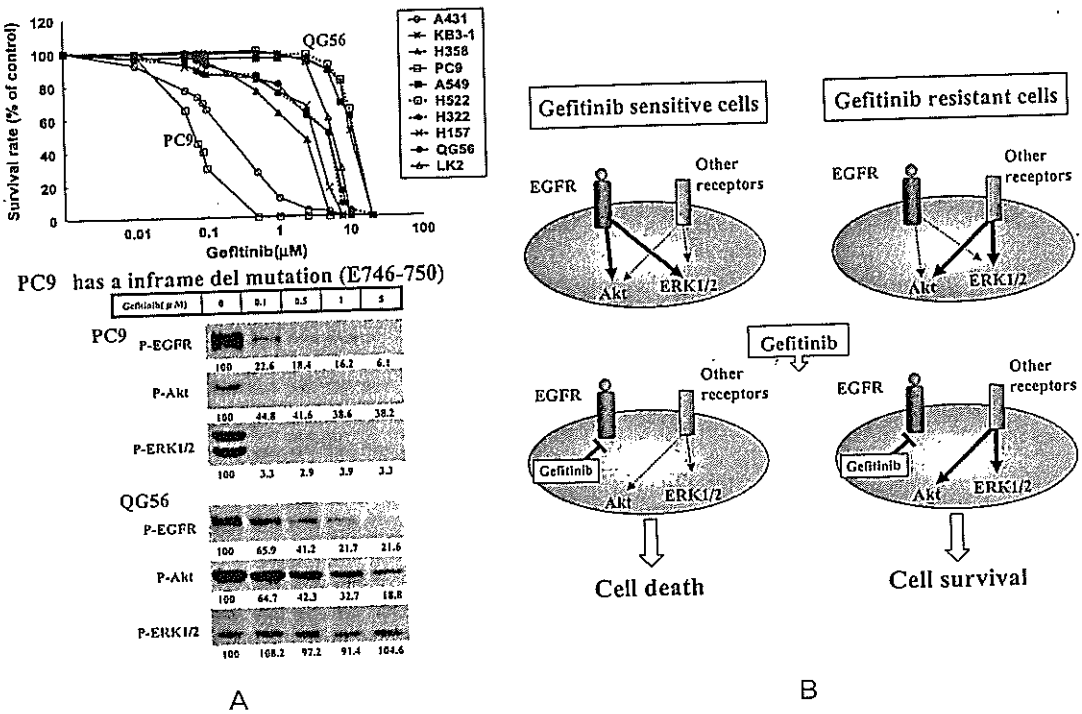

図5　A　ヒト肺癌細胞におけるゲフィチニブ感受性とシグナル伝達の阻害.
B　ヒト肺癌細胞におけるゲフィチニブ感受性はEGF/EGFレセプターに細胞死と増殖がどれだけ緊密に依存するかによって決められる.

謝　辞

本研究をまとめるにあたり山名秀明教授（先端癌治療研究センター長）をはじめ共同研究者の皆さんへ感謝します.

文　献

1）Taniguchi K, Wada M, Kohno K, Nakamura T, Kawakami M, Kagotani K, Okumura K, Akiyama S, Kuwano M：A human canalicular multispecific lroganic anion transporter (cMOAT) gene is overexpressed in cisplatin resistant human cancer cell lines with decreased drug accumulation. Cancer Res., 56：4124－4129, 1996

2）Wada M, Toh S, Taniguchi K, Uchiumi T, Kohno K, Yoshida I, Kimura A, Sakisaka S, Adachi Y, Kuwano M：Mutation in the canalicular multispecific organic anion transporter (cMOAT) gene, a novel ABC transporter, in patients with hyperbilirubinemia II / Dubin-Johnson syndrome. Human Molec. Genet., 7：203－207, 1998

3）Toh S, Wada M, Uchiumi T, Inokuchi A, Makino Y, Horie H, Adachi Y, Sakisaka S, Kuwano M：Genomic structure of the canalicular multispecitic organic anion transporter (cMOAT) gene and mutations in the ATP binding cassette region in Dubin-Johnson syndrome. Am. J. Human Genet., 64：739－746, 1999

4）Hashimoto K, Uchiumi T, Konno T, Ebihara T, Nakamura T, Wada M, Sakisaka S, Maniwa F, Amachi T, Ueda K, Kuwano M：Trafficking and functional defects by mutations of the ATP-binding domains in MRP2 in patients with Dubin-Johnson syndrome. Hepatology, 36：1236－1245, 2002

5）Kohno K, Izumi H, Uchiumi T,

Ashizuka M, Kuwano M : The pleiotropic functions of the Y-box-binding protein, YB-1. Bio Essays, 25 : 691 - 698, 2003 (review)

6) Kuwano M, Oda Y, Izumi H, Yang S-J, Uchiumi T, Iwamoto Y, Toi M, Fujii T, Yamana H, Kinoshita H, Kamura T, Tsuneyoshi M, Yasumoto K, Kohno K : The role of nuclear YB-1 as a global marker in drug resistance. Molec. Cancer Therapeut., 3 : 1458 - 1492, 2004 (review)

7) Hirata A, Ogawa S, Kometani T, Kuwano T, Naito S, Kuwano M, Ono M : ZD1839 (Iressa) induces anti-angiogenic effects through inhibition of epidermal growth factor receptor tyrosine kinase. Cancer Res., 62 : 2554 - 2560, 2002

8) Nakamura H, Takamori S, Fujii T, Ono M, Yamana H, Kuwano M, Shirouzu K : Cooperative cell-growth inhibition by combination treatment with ZD1839 (Iressa) and trastuzumab (Herceptin) in non-small-cell lung cancer. Cancer Lett., in press.

9) Ono M, Hirata A, Kometani T, Miyagawa M, Ueda S, Kinoshita H, Fujii T, Kuwano M : Sensitivity to gefitinib ('Iressa', ZD1839) in non-small cell lung cancer cell lines correlates with dependence on the epidermal growth factor (EGF) receptor / extracellular signal-regulated kinase 1/2 and EGF receptor/Akt pathway for proliferation. Molec. Cancer Therapeut., 3 : 465 - 472, 2004

10) Hirata A, Hosoi F, Ueda S, Miyagawa M, Naito S, Fujii T, Kuwano M, Ono M : HER2 Overexpression increases sensitivity to gefitinib, an EGF receptor tyrosine kinase inhibitor, through inhibition of HER2/HER3 heterodimer formation in lung cancer cells. Cancer Res., in press.

11) Okuda T, Higashi Y, Kokame K, Tanaka C, Kondoh H, Miyata T : *Ndrg1*-deficient mice exhibit a progressive demyelinating disorder of peripheral nerves. Mol. Cell. Biol., 24 : 3949 - 3956, 2004

12) Hirata K, Masuda K, Morikawa W, He J-W, Kuraoka A, Kuwano M, Kawabuchi M : N-myc downstream-regulated gene 1 expression in injured sciatic nerves. GLIA, 47 : 325 - 334, 2004

13) Masuda K, Ono M, Okamoto M, Morikawa W, Otsubo M, Migita T, Tsuneyoshi M, Okuda H, Shuin T, Naito S, Kuwano M : Downregulation of CAP43 gene by von Hippel-Lindau tumor suppressor protein in human renal cancer cells. Int. J. Cancer, 105 : 803 - 810, 2003

14) Nishie A, Masuda K, Otsubo M, Migita T, Tsuneyoshi M, Kohno K, Shuin T, Naito S, Ono M, Kuwano M : High expression of the Cap43 gene in infiltrating macrophages of human renal cell carcinomas. Clin. Cancer Res., 7 : 2145 - 2151, 2001

15) Kuwano T, Nakao S, Yamamoto H, Tsuneyoshi M, Yamamoto T, Kuwano M, Ono M : Cyclooxygenase 2 is a key enzyme for inflammatory cytokinase-induced angiogenesis. FASEB J., 18 : 300 - 310, 2004

16) Kuwano M, Basaki Y, Kuwano T, Nakano S, Oie S, Y N Kimura, Fujii T, Ono M : The critical role of inflammatory cell infiltration in tumor angiogenesis-a targest for antitumor drug development? In "New Angiogenesis Research" by Nova Science Publishers, Inc., New York, in press

巻頭言

癌の分子標的治療の進歩

桑野信彦

久留米大学先端癌治療研究センター分子外科部門教授

個々の細胞や細胞社会(組織や器官)の構造と機能に関する基礎研究は，癌の悪性形質獲得の分子的背景を把握するうえで大きく貢献してきた．個々の癌細胞増殖や細胞死に関与する増殖因子やサイトカインと受容体，ならびにそれらのシグナリングなどを標的として登場してきたのが分子標的薬剤である．分子標的薬剤の登場は，癌のベンチ研究をベッドサイドへ橋わたしできる可能性を秘めており，創薬研究の分野をかつてないほど魅力的かつ戦略的にしている．EGF 受容体を標的としたゲフィチニブ(イレッサ®)の肺癌治療に関する発表は，米国臨床腫瘍学会(ASCO)の会場を興奮させ拍手がなりやまなかったと聞いている．

近年，癌細胞と間質との応答が癌の悪性化の進展に重要な役割を果たしていることが注目されている．癌の増大のみならず，転移・浸潤・血管新生・リンパ管新生などにおける間質応答を担う標的を対象にした創薬研究の，これからの発展も期待したい．

分子標的治療薬の臨床応用の過程で，“予想しなかった発見や副作用”が報告されている．BCR-ABL を標的とするイマチニブが，KIT が責任遺伝子である消化器間質腫瘍にも効果を示すこと，ゲフィチニブが高感受性を示す肺癌の EGF 受容体の遺伝変異，メタロプロテアーゼ阻害薬投与後の関節や筋肉痛，また VEGF 抗体薬ベバシズマブと化学療法剤との併用の抗腫瘍効果など，臨床の現場からの情報を大切に学びフィードバックしていくことはきわめて大切である．

プロテインキナーゼ C の発見者西塚泰美先生(2004 年 11 月他界)は，いつも“誰もやらないことをやる”というメッセージを口にされていた．わが国発の分子標的治療薬の誕生を期待したい．